

Resonant interactions between Kelvin ship waves and ambient waves

QIANG ZHU[†], YUMING LIU AND DICK K. P. YUE[‡]

Department of Mechanical Engineering, Massachusetts Institute of Technology, Cambridge,
MA 02139, USA

(Received 31 January 2007 and in revised form 24 October 2007)

We consider the nonlinear interactions between the steady Kelvin waves behind an advancing ship and an (unsteady) ambient wave. It is shown that, for moderately steep ship waves and/or ambient waves, third-order (quartet) resonant interaction among the two wave systems could occur, leading to the generation of a new propagating wave along a specific ray in the Kelvin wake. The wave vector of the generated wave as well as the angle of the resonance ray are determined by the resonance condition and are functions of the ship forward speed and the wave vector of the ambient wave. To understand the resonance mechanism and the characteristics of the generated wave, we perform theoretical analyses of this problem using two related approaches. To obtain a relatively simple model in the form of a nonlinear Schrödinger (NLS) equation for the evolution of the resonant wave, we first consider a multiple-scale approach assuming locally discrete Kelvin wave components, with constant wave vectors but varying amplitudes along the resonance ray. This NLS model captures the key resonance mechanism but does not account for the detuning effect associated with the wave vector variation of Kelvin waves in the neighbourhood of the resonance ray. To obtain the full quantitative features and evolution characteristics, we also consider a more complete model based on Zakharov's integral equation applied in the context of a continuous wave vector spectrum. The resulting evolution equation can be reduced to an NLS form with, however, cross-ray variable coefficients, on imposing a narrow-band assumption valid in the neighbourhood of the resonance ray. As expected, the two models compare well when wave vector detuning is small, in the near wake close to the ray. To verify the analyses, direct high-resolution simulations of the nonlinear wave interaction problem are obtained using a high-order spectral method. The simulations capture the salient features of the resonance in the near wake of the ship, with good agreements with theory for the location of the resonance and the growth rate of the generated wave.

1. Introduction

Understanding of nonlinear resonant wave–wave interactions is important to the modelling and prediction of ocean wave dynamics, and to the interpretation and recognition of remotely sensed sea surface patterns. There have been a large number of theoretical, computational and experimental studies on the fundamental mechanisms of quartet and quintet resonant wave–wave interactions (e.g. Phillips 1960) and their

[†] Present address: Department of Structure Engineering, UCSD, USA

[‡] Author to whom correspondence should be addressed: yue@mit.edu

effects upon ocean wave field evolutions in deep water (e.g. Hasselmann *et al.* 1988) as well as in nearshore regions (e.g. Booij, Ris & Holthuijsen 1999; Liu & Yue 1998).

The extension of these studies to the case involving ship waves has been quite limited. In particular, the problem of nonlinear resonant interactions of ship waves with ambient waves has not been addressed. This is the subject of this paper. For a ship moving at a constant forward speed in a calm water, it is well known from classical linear theory (see e.g. Newman 1977) that the generated diverging and transverse waves are confined within a wedge of $\pm 19.5^\circ$ behind the ship. These waves are steady relative to the ship and the wave system is referred to as the Kelvin wake. When free-surface nonlinearity is included, it is shown (Newman 1971) that third-order quartet resonance does not occur among the diverging and transverse waves except near the cusp lines, where they merge into the same wave. By including third-order self-interactions, Akylas (1987) showed the presence of nonlinear steady-state (diverging or transverse) waves near the cusp lines, which is qualitatively similar to the classical linear result. These studies indicate that the steady ship waves even with high steepness are dominated by the (linear) Kelvin wake.

The present work is motivated in part by observations of large-scale persistent wave features within Kelvin ship wakes; for example, long, narrow V-shaped wave features in satellite pictures (e.g. Fu & Halt 1982; Shemdin 1987; Munk, Scully-Power & Zachariasen 1987; Reed & Milgram 2002), and oblique soliton-like wave envelopes observed in the field (Brown *et al.* 1988). Such narrow V-shaped and/or soliton-like wave patterns are of course not predicted by the classical Kelvin wave theory and a number of studies have been devoted to understanding their generation mechanisms. Peregrine (1971) found that narrow V-shaped waves can be generated due to refraction of stern waves by the viscous shear flow in the near wake of the ship. By modelling the ship waves as a result of combined effects of a source at the bow and a sink at the stern, Hall & Buchsbaum (1990) showed that steady rays can be formed inside the Kelvin wake. The positions of these rays as well as the wave vectors and strengths of waves at these rays are dependent on the forward speed, the bow-to-stern length, and the volume of the ship. If fluid stratification effect is considered, Tulin & Miloh (1990) showed that narrow, steady V-shaped surface wave features can be formed due to interactions with internal waves. Such features can also be due to unsteady effects such as those associated with high-frequency heave/pitch oscillations of a ship (Mei & Naciri 1991), general unsteady ship motions (Eggers & Schultz 1992), and turbulent wake near the stern (Munk *et al.* 1987). All these mechanisms primarily obtain in the context of linearized wave theory. The present investigation addresses the possible role of nonlinear interactions that might be present among the steady ship wave components and an ambient wave.

In this paper, we study the problem of nonlinear interactions of steady ship waves with an ambient wave. In particular, we address the following three questions.

- (a) Do steady ship waves interact resonantly with ambient waves?
- (b) If so, what are the order of interactions and the mechanism of resonances?
- (c) If so, what are the distinctive wave features in the ship wake associated with such nonlinear interactions?

By theoretical analysis based on both the cubic Schrödinger equation and Zakharov equation, we show that the (third-order) quartet resonant interactions of steady ship waves and a plane ambient wave can be developed along certain rays in the Kelvin wake of a ship. Under the resonance, a new propagating wave can be generated in the vicinity of the resonance ray. The position of the resonance ray and the basic characteristics of the generated wave can be determined from the resonance condition,

depending on ship forward speed and wave vector of ambient waves. Significantly, the generated wave possesses a distinctive solitary envelope across the resonance ray, which extends to a long distance from the ship. The present theoretical analysis is verified by a direct computation of the nonlinear interaction problem.

The paper is organized as follows. In §2, we summarize the general resonance conditions for third-order quartet resonant interaction between ship waves in a Kelvin wake and a plane ambient wave. To understand the resonance mechanism, we first apply, in §3.1, a multiple-scale analysis to derive the cubic Schrödinger equation for the evolution of the interacting wave components under the assumption of constant wave vectors for the Kelvin waves in the neighbourhood of the resonance ray. To account for the detuning effects on the resonance interactions due to spatial variations of wave vectors within the Kelvin wake, we develop in §3.2 a more complete model starting with the third-order Zakharov differential-integral equation. In §3.3, we show that the evolution equation in §3.2 can be reduced to an NLS form (with different variable coefficients) in the neighbourhood of the resonance ray when the characteristics of the ship waves and a narrow band assumption are applied. The features of the theoretical predictions are compared and discussed in §3.4. To verify the theoretical analysis, we perform direct numerical simulations of the nonlinear wave interaction problem in §4 using a high-order spectral method, and compare the computational results to theoretical prediction. In §5, the conclusion is drawn.

2. Resonance conditions

We consider a ship moving at a constant forward velocity U in deep water, in the presence of a plane progressive ambient wave, with the wave vector \mathbf{k}_i and frequency $\omega_i = (gk_i)^{1/2}$, where $k_i \equiv |\mathbf{k}_i|$ is the amplitude of the wave vector and g is the gravitational acceleration. Our interest is in the nonlinear resonant interactions between the steady (relative to the ship) wave components in the Kelvin wake and the (unsteady) ambient wave.

We define a space-fixed right-handed Cartesian coordinate system (O - XYZ) with the origin located on the mean free surface, the X -axis pointing in the direction of ship forward speed and Z -axis positive upward, as shown in figure 1. For convenience, we also define a ship-fixed coordinate system (O' - $X'Y'Z'$), which is related to the O - XYZ system by $X' = X - Ut$, $Y' = Y$ and $Z' = Z$, where t is time and $U \equiv |U|$ is the ship forward speed.

The Kelvin waves contain diverging and transverse waves whose far-field characteristics are well known (e.g. Newman 1977). For later convenience, the basic kinematics of waves in the Kelvin wake are briefly described here. Referring to the (space-fixed) O - XYZ system, both diverging and transverse waves are free propagating waves. The wave vectors, \mathbf{k}_d and \mathbf{k}_s , and the corresponding frequencies, ω_d and ω_s , satisfy the dispersion relation: $\omega_d = (gk_d)^{1/2}$ and $\omega_s = (gk_s)^{1/2}$, where $k_d \equiv |\mathbf{k}_d|$ and $k_s \equiv |\mathbf{k}_s|$. In the (ship-fixed) O' - $X'Y'Z'$ system, they become steady. The wave vectors \mathbf{k}_d and \mathbf{k}_s are constant along any ray given by $\tan \alpha = -Y'/X'$ for $X' < 0$, where α is measured clockwise from the track of the ship. Along the ray, we denote the propagating directions of \mathbf{k}_d and \mathbf{k}_s by θ_d and θ_s respectively, measured anti-clockwise from the direction of ship motion. These satisfy the equation (Newman 1977):

$$\tan \alpha = \frac{\sin \theta \cos \theta}{1 + \sin^2 \theta} \quad (2.1)$$

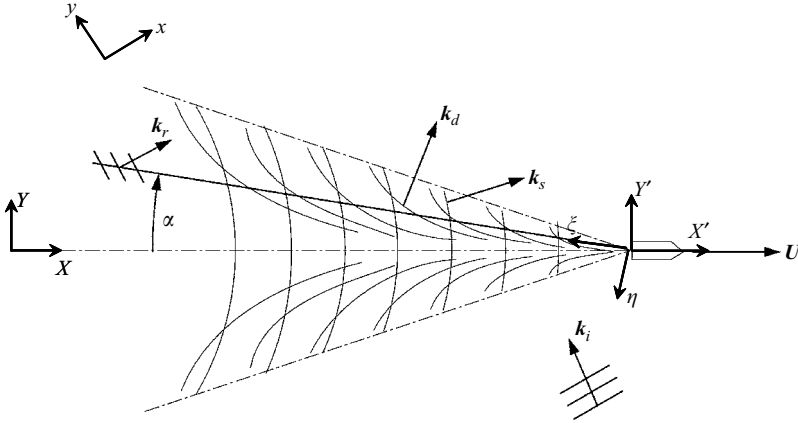


FIGURE 1. Cartesian coordinate systems used in the analysis and a sketch of a resonant quartet wave system formed by the Kelvin diverging (\mathbf{k}_d) and transverse (\mathbf{k}_s) waves of an advancing ship, the plane ambient incident wave (\mathbf{k}_i), and the resonance-generated wave (\mathbf{k}_r).

with $35.16^\circ \leq |\theta_d(\alpha)| \leq 90^\circ$ and $|\theta_s(\alpha)| \leq 35.16^\circ$. In terms of θ_d and θ_s , the magnitudes of \mathbf{k}_d and \mathbf{k}_s are given by

$$k_d(\alpha) = k_0 \sec^2 \theta_d \quad \text{and} \quad k_s(\alpha) = k_0 \sec^2 \theta_s \tag{2.2}$$

where $k_0 \equiv g/U^2$. Equation (2.1) possesses real roots for θ for $|\alpha| \leq 19.5^\circ$ only, so that the diverging and transverse waves appear only in the Kelvin wake within a wedge given by $|\alpha| \leq 19.5^\circ$.

It is well known that the leading-order resonance for nonlinear interactions of surface gravity waves in deep water can occur at third order (in the wave steepness) involving four wave components. The conditions for quartet resonant interactions of the waves in the Kelvin ship wake and the ambient plane incident wave can be deduced from the general resonance condition for nonlinear wave-wave interactions (e.g. Phillips 1960). Specifically, interactions among four different wave components become resonant at third order (in the wave steepness) if the wavenumbers \mathbf{k}_j and the corresponding frequencies satisfying the (deep-water) dispersion relationship, $\omega_j = (gk_j)^{1/2}$, $j = 1, 2, 3, 4$, satisfy

$$\mathbf{k}_1 + \mathbf{k}_2 = \mathbf{k}_3 + \mathbf{k}_4, \quad \omega_1 + \omega_2 = \omega_3 + \omega_4. \tag{2.3}$$

For convenience, we hereafter refer to the third-order resonance quartet given by the condition (2.3) as $[\mathbf{k}_1, \mathbf{k}_2, \mathbf{k}_3, \mathbf{k}_4]$. The conditions for third-order quartet resonance for the present problem involving a Kelvin wake and a plane incident wave are obtained by replacing the wave components (\mathbf{k}_j, ω_j) in (2.3) by the ambient incident wave (\mathbf{k}_i, ω_i) , the diverging wave (\mathbf{k}_d, ω_d) and the transverse wave (\mathbf{k}_s, ω_s) wave, and the resonance-generated wave $(\mathbf{k}_r, \omega_r = (g|\mathbf{k}_r|)^{1/2})$.

Since \mathbf{k}_d and \mathbf{k}_s are functions of α , a third-order resonance quartet can be formed only along a particular ray in the wake of the ship, which travels together with the ship. In order for the generated wave (\mathbf{k}_r) to grow, the \mathbf{k}_r wave must propagate in such a way that it remains on the resonance ray. This leads to an additional condition to be satisfied by the \mathbf{k}_r wave:

$$(\mathbf{C}_{gr} - \mathbf{U}) \cdot \mathbf{n} = 0, \quad \text{on} \quad \alpha = -\tan^{-1}(Y'/X'), \tag{2.4}$$

where $C_{gr} \equiv \omega_r k_r / (2k_r^2)$ is the group velocity of the k_r wave and \mathbf{n} is the unit normal vector of the resonance ray ($\alpha = -\tan^{-1}(Y'/X')$). If conditions (2.3) and (2.4) are satisfied, third-order resonant interaction among the k_i , k_d and k_s waves will result in a persistent resonant wave with wave vector k_r along the same ray. A sketch of such a quartet resonant wave system is shown in figure 1.

In general, the resonance (2.3) can be satisfied by the following three combinations of quartet wave vectors: (I) $k_1 = k_2 = k_3 = k_4$; (II) $k_1 = k_2 \neq k_3 \neq k_4$; and (III) $k_1 \neq k_2 \neq k_3 \neq k_4$. Case (I) is the simplest and occurs at third order in the Stokes expansion of a single plane progressive wavetrain. (II) corresponds to the case where two wave components in the quartet are identical. For plane progressive waves, Phillips (1960) studied this case and reduced the resonance condition (2.3) to the well-known 'figure of 8' diagram. Case (III) is the most general.

In the present investigation, both cases (II) and (III) must be considered. For case (II), there are four possible wave vector combinations which can form third-order resonant quartets: $[k_i, k_i, k_s, k_r]$; $[k_i, k_i, k_d, k_r]$; $[k_s, k_s, k_i, k_r]$; and $[k_d, k_d, k_i, k_r]$. Note that, according to Newman (1971), resonance quartet cannot be formed by $[k_s, k_s, k_d, k_r]$ or $[k_d, k_d, k_s, k_r]$. In addition, in this study we do not include the case with the generated wave k_r counted twice, for which the growth of the generated wave is much weaker than that in other wave vector combinations. For case (III), there are three possible resonant combinations: $[k_i, k_s, k_d, k_r]$; $[k_i, k_d, k_s, k_r]$; and $[k_i, k_r, k_s, k_d]$.

As an illustration of the above, we consider the resonance quartet, $[k_i, k_i, k_s, k_r]$, involving the incident ambient wave, ship transverse wave, and resonance-generated wave. The other cases involving ship diverging waves can be considered similarly, but are not shown here, for brevity. Let $k_1 = k_2 = k_i$, $k_3 = k_s$ and $k_4 = k_r$ and then (2.3) can be rewritten in the form (Phillips 1960):

$$\left. \begin{aligned} k_r &= \Lambda(2k_i - k_s), \\ \cos(\theta_i - \theta_s) &= 2\kappa^{1/2} + 8\kappa^{-1/2} - 3\kappa^{-1} - 6, \end{aligned} \right\} \quad (2.5)$$

where $\kappa = k_s/k_i$, and θ_i denotes the direction of k_i . In the above, $\Lambda = +1(-1)$ for $\kappa < (>)4$, which ensures $\omega_r > 0$. Upon using the first equation of (2.5), the condition (2.4) takes the form

$$\frac{\Lambda\kappa^{1/2}(2\sin\theta_i - \kappa\sin\theta_s)}{\Lambda\kappa^{1/2}(2\cos\theta_i - \kappa\cos\theta_s) - 2f^{3/2}/\cos\theta_s} = -\frac{\sin\theta_s \cos\theta_s}{1 + \sin^2\theta_s}, \quad (2.6)$$

where f is a function of κ , θ_i and θ_s :

$$f(\kappa, \theta_i, \theta_s) = [4 - 4\kappa \cos(\theta_i - \theta_s) + \kappa^2]^{1/2}. \quad (2.7)$$

The first equation of (2.5) gives k_r in terms of k_i and k_s , while (2.6) and the second equation of (2.5) provide the relation between k_i and k_s . For a given θ_s (or α), we solve for κ (i.e. $|k_i|$) and θ_i from (2.6) and the second equation of (2.5). From (2.6), it is clear that κ and θ_i are respectively even and odd functions of α .

For a given α , two independent sets of solutions for k_i and θ_i can be obtained: one has relatively small $k_r < k_i$; and the other a relatively large $k_r > k_i$. In figures 2 and 3, the two sets of solutions of k_i and θ_i and the resulting k_r and θ_r are shown as a function of α for $-19.5^\circ \leq \alpha \leq 19.5^\circ$. The conditions for each of the other resonant quartets (including the ones involving divergent waves) can be analysed in the same manner. For brevity, these results are not presented here (for details, see Zhu 2000). We note that numerical analyses of these conditions indicate that it is unlikely for multiple quartet resonances to obtain simultaneously for a given ambient wave.

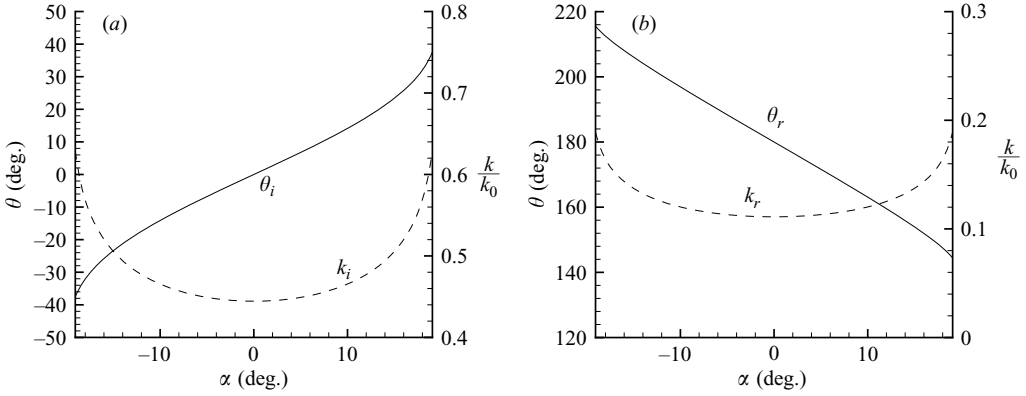


FIGURE 2. First solution of the resonance condition for the quartet interaction of the transverse ship wave (\mathbf{k}_s) and the plane ambient wave (\mathbf{k}_i), with the resonance-generated wave $\mathbf{k}_r = 2\mathbf{k}_i - \mathbf{k}_s$, along the ray α in the Kelvin wake of an advancing ship. (a) The amplitude k_i (---) and direction θ_i (—) of wave vector of the ambient incident wave. (b) The amplitude k_r (---) and direction θ_r (—) of wave vector of the resonance-generated wave as a function of α .

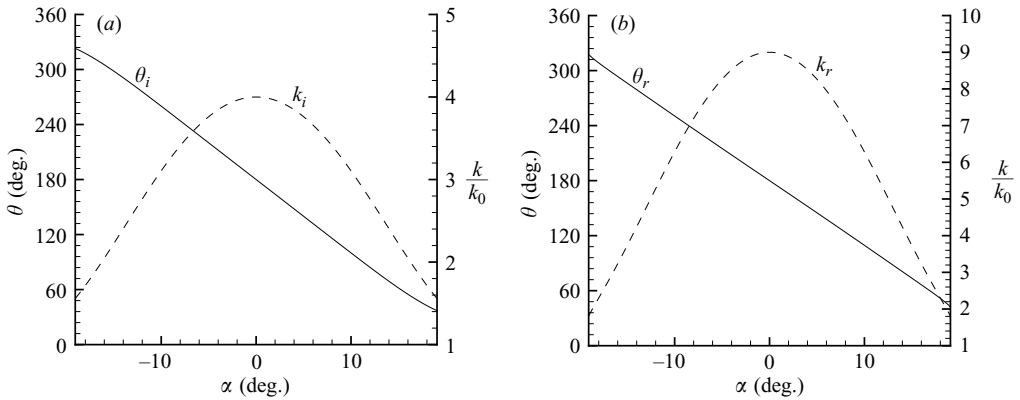


FIGURE 3. Second solution of the resonance condition for the quartet interaction of the transverse ship wave (\mathbf{k}_s) and the plane ambient wave (\mathbf{k}_i), with the resonance-generated wave $\mathbf{k}_r = 2\mathbf{k}_i - \mathbf{k}_s$, along the ray α in the Kelvin wake of an advancing ship. (a) The amplitude k_i (---) and direction θ_i (—) of wave vector of the ambient incident wave. (b) The amplitude k_r (---) and direction θ_r (—) of wave vector of the resonance-generated wave as a function of α .

3. Theoretical analysis

To understand the resonance mechanism and the features of the generated wave, in this section we perform theoretical analysis to derive the nonlinear evolution equations for the interacting wave components. In the analysis, two approaches are taken. The first one is a multiple-scale approach that accounts for the resonance effect on the resonance ray but neglects the detuning effect associated with the variation of wave vector of Kelvin waves across the ray. The resulting evolution equation, in the form of a cubic Schrödinger equation (e.g. Benny 1962; Mei, Stiassnie & Yue 2005), obtains the resonance on the resonance ray but strictly not in the neighbourhood of the ray. To capture the full nonlinear interactions in the Kelvin wake in the neighbourhood

of the resonance ray, we develop a second approach based on the Zakharov equation (e.g. Zakharov 1968; Crawford *et al.* 1981).

3.1. A cubic Schrödinger equation model based on locally constant wave vectors

In a preliminary analysis, the wave evolution on the resonance ray itself can be obtained using a multiple-scale analysis using the assumption that the ship waves behave locally like modulated amplitude plane waves with constant wave vector. Clearly, in this case, detuning effects associated with the spatial variation of wave vectors of Kelvin waves across the resonance ray are neglected. With this assumption, the analysis is similar to that for the quartet resonant interactions of plane waves (e.g. Benny 1962; Mei *et al.* 2005).

Using the resonance case with $\mathbf{k}_r = 2\mathbf{k}_i - \mathbf{k}_s$ as an example, we start by considering the evolution of the generated resonant wave \mathbf{k}_r . For convenience, we define another space-fixed Cartesian coordinate system $o - xyz$, with the x -axis pointing in the direction of \mathbf{k}_r and the z -axis upwards (see figure 1 and the Appendix for detail). In the context of potential flow, the wave motion is described by a velocity potential $\Phi(x, y, z, t)$. At any time, $\Phi(x, y, z, t)$ satisfies the Laplace equation within the fluid:

$$\Phi_{xx} + \Phi_{yy} + \Phi_{zz} = 0. \quad (3.1)$$

and the nonlinear kinematic and dynamic boundary conditions on the instantaneous free surface, $z = \zeta(\mathbf{x}, t)$, where $\mathbf{x} \equiv (x, y)$:

$$\left. \begin{aligned} \Phi_{tt} + g\Phi_z + 2\nabla\Phi \cdot \nabla\Phi_t + \frac{1}{2}\nabla\Phi \cdot \nabla(|\nabla\Phi|^2) &= 0, \\ \Phi_t + \frac{1}{2}|\nabla\Phi|^2 + g\zeta &= 0. \end{aligned} \right\} \quad (3.2)$$

In deep water, wave motion vanishes, i.e. $\nabla\Phi \rightarrow 0$ as $z \rightarrow -\infty$. This boundary-value problem for Φ governs the dynamics of the nonlinear wave-wave interactions. We now apply the multiple-scale procedure (e.g. Mei *et al.* 2005) to the boundary-value problem. As in Benny & Roskes (1969), we here consider the general case for which, in addition to slow time, slow spatial effects in both horizontal directions (x and y) are all accounted for.

On introducing slow space and time variables,

$$x_1 = \epsilon x, x_2 = \epsilon^2 x, \dots, \quad y_1 = \epsilon y, y_2 = \epsilon^2 y, \dots, \quad \text{and} \quad t_1 = \epsilon t, t_2 = \epsilon^2 t, \dots, \quad (3.3)$$

where $\epsilon \ll 1$ is a small parameter measuring the wave steepness, we expand the potential Φ and the surface elevation ζ in perturbation series:

$$\Phi = \sum_{n=1} \epsilon^n \phi^{(n)}(x, x_1, \dots; y, y_1, \dots; z; t, t_1, \dots), \quad (3.4)$$

$$\zeta = \sum_{n=1} \epsilon^n \zeta^{(n)}(x, x_1, \dots; y, y_1, \dots; t, t_1, \dots). \quad (3.5)$$

Substituting these expansions into (3.1) and (3.2), expanding the free-surface boundary conditions in Taylor series about the mean free surface $z=0$, and collecting terms at each order, we obtain a sequence of linear boundary-value problems for the perturbation potentials $\phi^{(n)}$ and free-surface elevations $\zeta^{(n)}$, for $n = 1, 2, \dots$:

$$\nabla^2 \phi^{(n)} = F^{(n)}, \quad z \leq 0, \quad (3.6)$$

$$\left(g \frac{\partial}{\partial z} + \frac{\partial^2}{\partial t^2} \right) \phi^{(n)} = G^{(n)}, \quad z = 0, \quad (3.7)$$

$$-g\zeta^{(n)} = H^{(n)}, \quad z = 0, \quad (3.8)$$

$$\nabla\phi^{(n)} \rightarrow 0 \quad \text{as } z \rightarrow -\infty. \quad (3.9)$$

In the above, the forcing terms $F^{(n)}$, $G^{(n)}$ and $H^{(n)}$ are explicitly given in terms of the perturbation potentials and wave elevations at lower orders. Their expressions (for $n \leq 3$) are given in the Appendix. These linear boundary-value problems can be successively solved up to the desired order starting from $n = 1$.

The first-order problem is the classical linear problem. For the resonance case with $\mathbf{k}_r = 2\mathbf{k}_i - \mathbf{k}_s$, we write $\zeta^{(1)}$ and $\phi^{(1)}$ as

$$\zeta^{(1)} = \frac{1}{2} [A_i(\mathbf{x}, t)e^{i(\mathbf{k}_i \cdot \mathbf{x} - \omega_i t)} + A_s(\mathbf{x}, t)e^{i(\mathbf{k}_s \cdot \mathbf{x} - \omega_s t)} + A_r(\mathbf{x}, t)e^{i(\mathbf{k}_r \cdot \mathbf{x} - \omega_r t)}] + \text{c.c.}, \quad (3.10)$$

$$\phi^{(1)} = -\frac{g}{2} \left[\frac{A_i(\mathbf{x}, t)}{\omega_i} e^{i(\mathbf{k}_i \cdot \mathbf{x} - \omega_i t)} + \frac{A_s(\mathbf{x}, t)}{\omega_s} e^{i(\mathbf{k}_s \cdot \mathbf{x} - \omega_s t)} + \frac{A_r(\mathbf{x}, t)}{\omega_r} e^{i(\mathbf{k}_r \cdot \mathbf{x} - \omega_r t)} \right] + \text{c.c.}, \quad (3.11)$$

where A_i , A_s and A_r are the complex amplitudes of the ambient wave, the transverse ship wave, and the resonance-generated wave, respectively. In the above, $i \equiv (-1)^{1/2}$, and c.c. represents the complex conjugate of the previous terms. The wave amplitudes (A_i , A_s and A_r) depend on slow spatial and temporal variables: x_1, y_1, t_1, \dots

The equations governing the evolution of A_i , A_s , and A_r are obtained from the higher-order problems. For quartet resonance, the (leading-order) nonlinear evolution equations for A_i , A_s , and A_r are obtained based on the second-order solution $\phi^{(2)}$ and $\zeta^{(2)}$ and the solvability condition for $\phi^{(3)}$. The derivation is quite involved, but straightforward, and is omitted here (the key steps are outlined in the Appendix). The evolution equation for the amplitude of the resonance-generated wave can be finally expressed in the form of a cubic nonlinear Schrödinger equation (NLS) involving cubic nonlinear interactions among the incident, transverse and the generated resonant waves:

$$\begin{aligned} & \left[i \frac{\partial}{\partial t} + C_{gr} \left(i \frac{\partial}{\partial x} - \frac{1}{4k_r} \frac{\partial^2}{\partial x^2} + \frac{1}{2k_r} \frac{\partial^2}{\partial y^2} \right) \right] A_r \\ & = C_{rsii} A_i^2 A_s^* + C_{rrrr} A_r^* A_r^2 + C_{riri} A_i^* A_i A_r + C_{rsrs} A_s^* A_s A_r, \end{aligned} \quad (3.12)$$

where the coefficients C_{rsii} , C_{rrrr} , C_{riri} and C_{rsrs} are ultimately functions of \mathbf{k}_i , \mathbf{k}_s and \mathbf{k}_r , and are constants in the entire resonance region considered. The evolution equations for A_i and A_s are obtained similarly, based on the analysis in the Appendix, but are not shown here, for brevity. The three coupled evolution equations are solved together to determine the variation of the amplitudes of interacting waves.

Note that in the above analysis we assume homogeneous conditions, i.e. plane progressive wave components satisfying resonance condition in the absence of other waves. The NLS (3.12) is thus valid only on the resonance ray as the analysis here does not take into account the fact that the wave vector of ship waves varies continuously across the resonance ray. In particular, the effect of detuning away from the resonance ray (e.g. Li & Tulin 1999) is neglected. The extension to include the true inhomogeneous condition in the NLS context is not straightforward. For a complete treatment including these effects, in the following section we perform an analysis based on the Zakharov equation to account for the nonlinear interactions in a continuous spectrum including both resonance and near-resonance effects (see e.g. Zakharov 1968; Crawford *et al.* 1981).

3.2. A complete model based on the Zakharov equation

To obtain the nonlinear resonant interactions involving varying wave components in the Kelvin wake, a general model can be derived starting from the Zakharov equation (e.g. Mei *et al.* 2005). According to Krasitskii (1994), the integral equation governing the nonlinear evolution of a wave component (\mathbf{k}_1), in a wave spectrum including third-order quartet resonant wave-wave interactions, can be written as

$$i \frac{\partial B(\mathbf{k}_1, t)}{\partial t} = \int \int \int_{-\infty}^{\infty} T(\mathbf{k}_1, \mathbf{k}_2, \mathbf{k}_3, \mathbf{k}_4) B^*(\mathbf{k}_2, t) B(\mathbf{k}_3, t) B(\mathbf{k}_4, t) \times \delta(\mathbf{k}_1 + \mathbf{k}_2 - \mathbf{k}_3 - \mathbf{k}_4) \exp[i(\omega_1 + \omega_2 - \omega_3 - \omega_4)t] d\mathbf{k}_2 d\mathbf{k}_3 d\mathbf{k}_4, \quad (3.13)$$

where * denotes complex conjugate and δ is the delta function. The dependent variable $B(\mathbf{k}, t)$ is related to the (Fourier) modal amplitudes of the wave elevation $\hat{\zeta}(\mathbf{k}, t)$ and the free-surface potential $\hat{\phi}^s(\mathbf{k}, t)$:

$$B(\mathbf{k}, t) = \left[\left(\frac{g}{2\omega(\mathbf{k})} \right)^{1/2} \hat{\zeta}(\mathbf{k}, t) + i \left(\frac{\omega(\mathbf{k})}{2g} \right)^{1/2} \hat{\phi}^s(\mathbf{k}, t) \right] e^{i\omega(\mathbf{k})t}. \quad (3.14)$$

The kernel T accounts for the quartet interaction effect of waves \mathbf{k}_1 , \mathbf{k}_2 , \mathbf{k}_3 , and \mathbf{k}_4 takes the form

$$T(\mathbf{k}_1, \mathbf{k}_2, \mathbf{k}_3, \mathbf{k}_4) = (Z_{1,2,3,4} + Z_{2,1,3,4} + Z_{3,4,1,2} + Z_{4,3,1,2})/4 + W_{1,2,3,4}, \quad (3.15)$$

where

$$Z_{1,2,3,4} = -\frac{2V_{4,4-2,2}^{(-)} V_{1,3,1-3}^{(-)}}{\omega_{2-4} - \omega_4 + \omega_2} - \frac{2V_{3,1,3-1}^{(-)} V_{2,2-4,4}^{(-)}}{\omega_{2-4} - \omega_2 + \omega_4} - \frac{2V_{3,3-2,2}^{(-)} V_{1,4,1-4}^{(-)}}{\omega_{2-3} - \omega_3 + \omega_2} - \frac{2V_{4,1,4-1}^{(-)} V_{2,2-3,3}^{(-)}}{\omega_{2-3} - \omega_2 + \omega_3} - \frac{2V_{1+2,1,2}^{(-)} V_{3+4,3,4}^{(-)}}{\omega_{3+4} - \omega_3 - \omega_4} - \frac{2V_{-3-4,3,4}^{(+)} V_{1,2,-1-2}^{(+)}}{\omega_{3+4} + \omega_3 + \omega_4}, \quad (3.16)$$

$$V_{1,2,3}^{(\pm)} = \frac{1}{8\pi\sqrt{2}} \left\{ (\mathbf{k}_1 \cdot \mathbf{k}_2 \pm k_1 k_2) \left(\frac{\omega_1 \omega_2}{\omega_3} \frac{k_3}{k_1 k_2} \right)^{1/2} + (\mathbf{k}_1 \cdot \mathbf{k}_3 \pm k_1 k_3) \left(\frac{\omega_1 \omega_3}{\omega_2} \frac{k_2}{k_1 k_3} \right)^{1/2} + (\mathbf{k}_2 \cdot \mathbf{k}_3 \pm k_2 k_3) \left(\frac{\omega_2 \omega_3}{\omega_1} \frac{k_1}{k_2 k_3} \right)^{1/2} \right\}, \quad (3.17)$$

$$W_{1,2,3,4} = \bar{W}_{-1,-2,3,4} + \bar{W}_{3,4,-1,-2} - \bar{W}_{3,-2,-1,4} - \bar{W}_{-1,3,-2,4} - \bar{W}_{-1,4,3,-2} - \bar{W}_{4,-2,3,-1}, \quad (3.18)$$

$$\bar{W}_{1,2,3,4} = \frac{1}{64\pi^2} \left[\frac{\omega_1 \omega_2}{\omega_3 \omega_4} k_1 k_2 k_3 k_4 \right]^{1/2} [2(k_1 + k_2) - k_{2+4} - k_{2+3} - k_{1+4} - k_{1+3}], \quad (3.19)$$

and

$$k_{i\pm j} = |\mathbf{k}_i \pm \mathbf{k}_j|, \quad \omega_{i\pm j} = \omega(\mathbf{k}_{i\pm j}).$$

Applying (3.13) to the present problem involving the Kelvin ship wake and ambient wave components, we obtain, for the resonance case $[\mathbf{k}_i, \mathbf{k}_i, \mathbf{k}_s, \mathbf{k}_r]$, the following evolution equation for the resonance-generated wave:

$$i \frac{\partial B_r(\mathbf{k}_1, t)}{\partial t} = \int \int \int_{-\infty}^{\infty} T(\mathbf{k}_1, \mathbf{k}_2, \mathbf{k}_3, \mathbf{k}_4) B_s^*(\mathbf{k}_2, t) B_i(\mathbf{k}_3, t) B_i(\mathbf{k}_4, t) \times \delta(\mathbf{k}_1 + \mathbf{k}_2 - \mathbf{k}_3 - \mathbf{k}_4) \exp[i(\omega_1 + \omega_2 - \omega_3 - \omega_4)t] d\mathbf{k}_2 d\mathbf{k}_3 d\mathbf{k}_4$$

$$\begin{aligned}
& + \int \int \int_{-\infty}^{\infty} T(\mathbf{k}_1, \mathbf{k}_2, \mathbf{k}_3, \mathbf{k}_4) B_r^*(\mathbf{k}_2, t) B_r(\mathbf{k}_3, t) B_r(\mathbf{k}_4, t) \\
& \times \delta(\mathbf{k}_1 + \mathbf{k}_2 - \mathbf{k}_3 - \mathbf{k}_4) \exp[i(\omega_1 + \omega_2 - \omega_3 - \omega_4)t] d\mathbf{k}_2 d\mathbf{k}_3 d\mathbf{k}_4 \\
& + 2 \int \int \int_{-\infty}^{\infty} T(\mathbf{k}_1, \mathbf{k}_2, \mathbf{k}_3, \mathbf{k}_4) B_i^*(\mathbf{k}_2, t) B_i(\mathbf{k}_3, t) B_r(\mathbf{k}_4, t) \\
& \times \delta(\mathbf{k}_1 + \mathbf{k}_2 - \mathbf{k}_3 - \mathbf{k}_4) \exp[i(\omega_1 + \omega_2 - \omega_3 - \omega_4)t] d\mathbf{k}_2 d\mathbf{k}_3 d\mathbf{k}_4 \\
& + 2 \int \int \int_{-\infty}^{\infty} T(\mathbf{k}_1, \mathbf{k}_2, \mathbf{k}_3, \mathbf{k}_4) B_s^*(\mathbf{k}_2, t) B_s(\mathbf{k}_3, t) B_r(\mathbf{k}_4, t) \\
& \times \delta(\mathbf{k}_1 + \mathbf{k}_2 - \mathbf{k}_3 - \mathbf{k}_4) \exp[i(\omega_1 + \omega_2 - \omega_3 - \omega_4)t] d\mathbf{k}_2 d\mathbf{k}_3 d\mathbf{k}_4, \quad (3.20)
\end{aligned}$$

where B_r , B_s , and B_i refer respectively to the resonance-generated, ship, and ambient waves. The first term on the right-hand side of (3.20) accounts for the effect of quartet resonance with $\mathbf{k}_r = 2\mathbf{k}_i - \mathbf{k}_s$. The other three terms represent the effects due to self-interaction with $\mathbf{k}_r = 2\mathbf{k}_r - \mathbf{k}_r$, and trivial quartet resonances with $\mathbf{k}_r = \mathbf{k}_r + \mathbf{k}_i - \mathbf{k}_i$ and $\mathbf{k}_r = \mathbf{k}_r + \mathbf{k}_s - \mathbf{k}_s$. Similar evolution equations for B_s and B_i can be obtained, but are not shown here for brevity.

Equation (3.20) gives a description of the nonlinear interactions among waves in a continuous spectrum (including ship and ambient waves). In the present context, the ship wave system is given as a superposition of free plane waves represented by $B_s(\mathbf{k}, t)$. The classical far-field Kelvin wake with spatially varying amplitudes can be obtained from this system by stationary phase analysis (e.g. Newman 1977). It is important to remark that the Zakharov equation is applied directly to the original general wave system and not to the varying amplitude Kelvin waves.

3.3. Simplification of the evolution equations

Unlike the cubic Schrödinger equation, (3.20) is in an integral form and difficult to resolve numerically. If our interest is in the neighbourhood of the resonance ray, (3.20) can be simplified using a narrow-band assumption. The final result can be expressed as a partial differential equation, which resembles in form the nonlinear Schrödinger equation (3.12). Unlike (3.12), this equation now includes the detuning effect not accounted for in the NLS.

In a small region around a resonance ray ($\alpha = \alpha_0$), we assume that the ship wave, ambient wave, and resonance-generated wave are narrow-banded around their corresponding central wave vectors \mathbf{k}_{s_0} , \mathbf{k}_i and \mathbf{k}_r , and write

$$\mathbf{k}_1 = \mathbf{k}_r + \mathbf{p}_1, \quad \mathbf{k}_2 = \mathbf{k}_{s_0} + \mathbf{p}_2, \quad \mathbf{k}_3 = \mathbf{k}_i + \mathbf{p}_3, \quad \mathbf{k}_4 = \mathbf{k}_i + \mathbf{p}_4, \quad (3.21)$$

where $|\mathbf{p}_1|/|\mathbf{k}_r|$, $|\mathbf{p}_2|/|\mathbf{k}_{s_0}|$, $|\mathbf{p}_3|/|\mathbf{k}_i|$, $|\mathbf{p}_4|/|\mathbf{k}_i| = o(1)$. This approximation allows (3.20) to be reduced to a simplified differential equation form. For clarity, we show the detailed steps of the simplification for the term involving $B_s^* B_i B_i$ only, and provide the final results for the other three terms involving $B_r^* B_r B_r$, $B_i^* B_i B_r$, and $B_s^* B_s B_r$. On substituting (3.21) into (3.20), we have

$$\begin{aligned}
& i \frac{\partial \tilde{B}_r(\mathbf{p}_1, t)}{\partial t} - [\omega(\mathbf{k}_r + \mathbf{p}_1) - \omega(\mathbf{k}_r)] \tilde{B}_r(\mathbf{p}_1, t) \\
& = \int \int \int_{-\infty}^{\infty} T(\mathbf{k}_r + \mathbf{p}_1, \mathbf{k}_{s_0} + \mathbf{p}_2, \mathbf{k}_i + \mathbf{p}_3, \mathbf{k}_i + \mathbf{p}_4) \\
& \quad \times \tilde{B}_s^*(\mathbf{p}_2, t) \tilde{B}_i(\mathbf{p}_3, t) \tilde{B}_i(\mathbf{p}_4, t) \delta(\mathbf{p}_1 + \mathbf{p}_2 - \mathbf{p}_3 - \mathbf{p}_4) d\mathbf{p}_2 d\mathbf{p}_3 d\mathbf{p}_4, \quad (3.22)
\end{aligned}$$

in which

$$\begin{aligned}\tilde{B}_r(\mathbf{p}_1, t) &\equiv B_r(\mathbf{k}_r + \mathbf{p}_1, t) \exp\{-i[\omega(\mathbf{k}_r + \mathbf{p}_1) - \omega(\mathbf{k}_r)]t\}, \\ \tilde{B}_s(\mathbf{p}_2, t) &\equiv B_s(\mathbf{k}_{s_0} + \mathbf{p}_2, t) \exp\{-i[\omega(\mathbf{k}_{s_0} + \mathbf{p}_2) - \omega(\mathbf{k}_{s_0})]t\}, \\ \tilde{B}_i(\mathbf{p}_3, t) &\equiv B_i(\mathbf{k}_i + \mathbf{p}_3, t) \exp\{-i[\omega(\mathbf{k}_i + \mathbf{p}_3) - \omega(\mathbf{k}_i)]t\}, \\ \tilde{B}_i(\mathbf{p}_4, t) &\equiv B_i(\mathbf{k}_i + \mathbf{p}_4, t) \exp\{-i[\omega(\mathbf{k}_i + \mathbf{p}_4) - \omega(\mathbf{k}_i)]t\}.\end{aligned}$$

Upon expanding $\omega(\mathbf{k}_r + \mathbf{p}_1)$ about $\mathbf{k} = \mathbf{k}_r$, we obtain

$$\omega(\mathbf{k}_r + \mathbf{p}_1) - \omega(\mathbf{k}_r) = C_{gr} \left(p_{1x} - \frac{p_{1x}^2}{4k_r} + \frac{p_{1y}^2}{2k_r} \right) + O(|\mathbf{p}_1|^3), \quad (3.23)$$

where $\mathbf{p}_1 \equiv (p_{1x}, p_{1y})$, with p_{1x} being the component of \mathbf{p}_1 in the direction of \mathbf{k}_r .

Applying the inverse Fourier transform to (3.22) and using (3.23), we obtain from the left-hand side of (3.22)

$$\mathcal{L} = i \frac{\partial a_r}{\partial t} + C_{gr} \left(i \frac{\partial a_r}{\partial x} - \frac{1}{4k_r} \frac{\partial^2 a_r}{\partial x^2} + \frac{1}{2k_r} \frac{\partial^2 a_r}{\partial y^2} \right) + O(|\mathbf{p}_1|^2), \quad (3.24)$$

where a_r is the inverse Fourier transform of \tilde{B}_r :

$$a_r(\mathbf{x}, t) = \frac{1}{2\pi} \int_{-\infty}^{\infty} \tilde{B}_r(\mathbf{p}_1, t) e^{i\mathbf{p}_1 \cdot \mathbf{x}} d\mathbf{p}_1. \quad (3.25)$$

Here $\mathbf{x} \equiv (x, y)$, with the x -axis pointing in the direction of \mathbf{k}_r . It is apparent from (3.14) that a_r is related to the amplitudes of wave elevation and free-surface potential of the resonance-generated wave. From the right-hand side of (3.22), we obtain

$$\begin{aligned}\mathcal{R} &\equiv \frac{1}{2\pi} \int_{-\infty}^{\infty} d\mathbf{p}_1 e^{i\mathbf{p}_1 \cdot \mathbf{x}} \int \int \int_{-\infty}^{\infty} T(\mathbf{k}_r + \mathbf{p}_1, \mathbf{k}_{s_0} + \mathbf{p}_2, \mathbf{k}_i + \mathbf{p}_3, \mathbf{k}_i + \mathbf{p}_4) \\ &\quad \times \tilde{B}_s^*(\mathbf{p}_2, t) \tilde{B}_i(\mathbf{p}_3, t) \tilde{B}_i(\mathbf{p}_4, t) \delta(\mathbf{p}_1 + \mathbf{p}_2 - \mathbf{p}_3 - \mathbf{p}_4) d\mathbf{p}_2 d\mathbf{p}_3 d\mathbf{p}_4 \\ &= \frac{1}{2\pi} \int \int \int_{-\infty}^{\infty} T(\mathbf{k}_r - \mathbf{p}_2 + \mathbf{p}_3 + \mathbf{p}_4, \mathbf{k}_{s_0} + \mathbf{p}_2, \mathbf{k}_i + \mathbf{p}_3, \mathbf{k}_i + \mathbf{p}_4) \\ &\quad \times \tilde{B}_s^*(\mathbf{p}_2, t) \tilde{B}_i(\mathbf{p}_3, t) \tilde{B}_i(\mathbf{p}_4, t) e^{i(-\mathbf{p}_2 + \mathbf{p}_3 + \mathbf{p}_4) \cdot \mathbf{x}} d\mathbf{p}_2 d\mathbf{p}_3 d\mathbf{p}_4.\end{aligned} \quad (3.26)$$

To leading order, the wave vector of the ambient wave can be considered to be constant in the neighbourhood of the resonance ray ($\alpha = \alpha_0$). Thus, \tilde{B}_i should behave like a δ function. As a result, upon neglecting the high-order effects for \tilde{B}_i , we obtain

$$\mathcal{R} = 2\pi a_i^2 \int_{-\infty}^{\infty} T(\mathbf{k}_r - \mathbf{p}_2, \mathbf{k}_{s_0} + \mathbf{p}_2, \mathbf{k}_i, \mathbf{k}_i) \tilde{B}_s^*(\mathbf{p}_2, t) e^{-i\mathbf{p}_2 \cdot \mathbf{x}} d\mathbf{p}_2, \quad (3.27)$$

where a_i is the inverse Fourier transform of \tilde{B}_i , which is related to the wave elevation and free-surface potential of the ambient incident wave.

The integral in (3.27) represents the contribution from all components of the ship wave system. As in the classical Kelvin solution (e.g. Newman 1977), this can be approximated using the method of stationary phase. In the far field, for the resonance considered here, this integral is dominated by contribution from the transverse wave component. We thus obtain

$$\mathcal{R} = 4\pi^2 T(\mathbf{k}_r - \mathbf{k}_s(X'), \mathbf{k}_{s_0}, \mathbf{k}_s(X'), \mathbf{k}_i, \mathbf{k}_i) a_i^2 a_s^*(X'), \quad (3.28)$$

where $X' \equiv (X', Y')$ in the ship-fixed coordinate system $O' - X'Y'Z'$ (see figure 1), and a_s is related to the wave elevation and free-surface potential of the transverse ship

wave component with wave vector $\mathbf{k}_s(X')$. (Note that in this context, a_s and \tilde{B}_s are not direct Fourier transforms of each other.)

The other three terms on the right-hand side of (3.20) can be simplified in a similar manner. Upon adding these contributions to \mathcal{R} , we obtain the simplified version of the evolution equation (3.20):

$$\left[i \frac{\partial}{\partial t} + C_{gr} \left(i \frac{\partial}{\partial x} - \frac{1}{4k_r} \frac{\partial^2}{\partial x^2} + \frac{1}{2k_r} \frac{\partial^2}{\partial y^2} \right) \right] a_r = 4\pi^2 (T_{rsii} a_i^2 a_s^* + T_{rrrr} a_r^* a_r^2 + 2T_{riri} a_i^* a_i a_r + 2T_{rsrs} a_s^* a_s a_r), \quad (3.29)$$

where $T_{rsii} = T(\mathbf{k}_r - \mathbf{k}_s + \mathbf{k}_{s0}, \mathbf{k}_s, \mathbf{k}_i, \mathbf{k}_i)$, $T_{rrrr} = T(\mathbf{k}_r, \mathbf{k}_r, \mathbf{k}_r, \mathbf{k}_r)$, $T_{riri} = T(\mathbf{k}_r, \mathbf{k}_i, \mathbf{k}_r, \mathbf{k}_i)$ and $T_{rsrs} = T(\mathbf{k}_r, \mathbf{k}_s, \mathbf{k}_r, \mathbf{k}_s)$. We note that (3.29) has a similar form to the cubic Schrödinger equation (3.12), obtained using multiple-scale analysis, assuming a constant wave vector across the resonance ray. Unlike (3.12), the coefficients T_{rsii}, \dots , in (3.29) now vary across the resonance ray and depend on the wave vector of the waves in the ship wake. Equation (3.29) can be considered as an extension of (3.12), with the inclusion of the detuning effect of near-resonance interactions across the resonance ray. At exact resonance, (3.29) recovers (3.12). We also remark that this detuning effect may be considered in §3.1 by introducing an additional scale associated with the variation of the wave vectors around the resonance ray. The analysis here based on the Zakharov equation turns out to be more straightforward.

Following a similar procedure, the simplified evolution equations for the ambient incident and ship waves in the neighbourhood of the resonance ray ($\alpha = \alpha_0$) can be obtained:

$$\left[i \frac{\partial}{\partial t} + C_{gi} \left(i \frac{\partial}{\partial x} - \frac{1}{4k_i} \frac{\partial^2}{\partial x^2} + \frac{1}{2k_i} \frac{\partial^2}{\partial y^2} \right) \right] a_i = 4\pi^2 (2T_{iirs} a_i^* a_r a_s + T_{iiii} a_i^* a_i^2 + 2T_{isis} a_s^* a_s a_i + 2T_{irir} a_i^* a_r a_i) \quad (3.30)$$

and

$$\left[i \frac{\partial}{\partial t} + C_{gs} \left(i \frac{\partial}{\partial x} - \frac{1}{4k_s} \frac{\partial^2}{\partial x^2} + \frac{1}{2k_s} \frac{\partial^2}{\partial y^2} \right) \right] a_s = 4\pi^2 (2T_{srri} a_i^2 a_r^* + T_{ssss} a_s^* a_s^2 + 2T_{sisi} a_i^* a_i a_s + 2T_{srss} a_r^* a_r a_s), \quad (3.31)$$

where C_{gi} and C_{gs} are the group velocities of the ambient incident wave and the transverse ship wave, respectively, at the resonant ray ($\alpha = \alpha_0$). The coefficients T_{srri}, \dots , are defined in the same way as those in (3.29). The Cartesian coordinates (x, y) in (3.30) and (3.31) are defined with the x -coordinate pointing in the direction of \mathbf{k}_i and \mathbf{k}_s , respectively.

3.4. Solution of the evolution equations

Here we solve (3.29)–(3.31) for the evolution of a_r , a_i and a_s . For convenience, we define a right-handed ship-fixed Cartesian coordinate system ($O' - \xi\eta Z'$), with the ξ -axis coincident with the resonance ray pointing away from the ship, and Z' positive upwards.

Referring to this coordinate system, and dropping the time-dependent term in (3.29) for the steady-state solution, we obtain, for the resonant wave,

$$\left(\sigma_1 \frac{\partial}{\partial \xi} + \sigma_2 \frac{\partial}{\partial \eta} \right) a_r + i \frac{\omega_r}{8k_r^2} \left(\sigma_3 \frac{\partial^2}{\partial \xi^2} + \sigma_4 \frac{\partial^2}{\partial \xi \partial \eta} + \sigma_5 \frac{\partial^2}{\partial \eta^2} \right) a_r + i4\pi^2 (T_{rsii} a_i^2 a_r^* + T_{rrrr} |a_r|^2 a_r + 2T_{riri} |a_i|^2 a_r + 2T_{rsrs} |a_s|^2 a_r) = 0. \quad (3.32)$$

In the above, the coefficients σ_j , $j = 1, \dots, 5$, result from the transformation of the coordinate system from $O - XYZ$ to $O' - \xi\eta Z'$, and are given by

$$\left. \begin{aligned} \sigma_1 &= U \cos \alpha - C_{g_r} \cos(\alpha + \theta_r), \\ \sigma_2 &= U \sin \alpha - C_{g_r} \sin(\alpha + \theta_r), \\ \sigma_3 &= \cos^2(\alpha + \theta_r) - 2 \sin^2(\alpha + \theta_r), \\ \sigma_4 &= 3 \sin 2(\alpha + \theta_r), \\ \sigma_5 &= \sin^2(\alpha + \theta_r) - 2 \cos^2(\alpha + \theta_r). \end{aligned} \right\} \quad (3.33)$$

Because of condition (2.4), the coefficient $\sigma_2 = 0$.

We now apply a simple finite-difference numerical scheme using a prediction–correction algorithm (Yue & Mei 1980) to solve (3.32), coupled with the evolution equations for the ship wave (a_s) and the ambient wave (a_i) (cf. (3.30) and (3.31)). The ambient incident wave steepness $k_i|A_i| \equiv \epsilon$ is used as a measure of nonlinearity in the resonant interaction. In the numerical calculations, the interaction coefficient $T(\mathbf{k}_1, \mathbf{k}_2, \mathbf{k}_3, \mathbf{k}_4)$ is computed using (3.15) if $|\omega_1 + \omega_2 - \omega_3 - \omega_4|/\omega < \epsilon^2$, and is otherwise set to be zero since the contribution of wave components further away from the resonance are negligibly small. Since steady ship waves even with high steepness are dominated by the linear Kelvin wake (Akylas 1987), we employ the Kelvin solution of the undisturbed ship wake for the wave associated with \mathbf{k}_s :

$$a_{s0}(\xi, \eta) = a_0 \left(\frac{\xi_0}{|\mathbf{X}'|} \right)^{1/2} e^{i[\mathbf{k}_s(\xi, \eta) - \mathbf{k}_s(\xi, 0)] \cdot \mathbf{X}'}, \quad \xi > \xi_0, \quad (3.34)$$

where $\mathbf{X}' \equiv (X', Y')$ represents the position of the point (ξ, η) in the ship-fixed coordinate system $O' - X'Y'Z'$, and $a_0 \equiv a_{s0}(\xi_0, \eta = 0)$. The value of a_0 depends on ship geometry and forward speed U . To ensure that the evolution equation (3.31) allows the particular Kelvin solution (3.34), we add a forcing term P to the right-hand side of (3.31) in the computation:

$$P(\mathbf{X}', t) \equiv \left[i \frac{\partial}{\partial t} + C_{g_s} \left(i \frac{\partial}{\partial x} - \frac{1}{4k_s} \frac{\partial^2}{\partial x^2} + \frac{1}{2k_s} \frac{\partial^2}{\partial y^2} \right) \right] a_{s0} - 4\pi^2 T_{ssss} |a_{s0}|^2 a_{s0}. \quad (3.35)$$

We obtain numerical results in a narrow strip centred around the resonance ray $\xi > \xi_0$ and $-\eta_0 < \eta < \eta_0$, and assume that the resonance interaction starts at $\xi = \xi_0 > 0$. On the transverse upstream boundary $\xi = \xi_0$, we set $a_r = 0$, $a_s = a_{s0}(\xi_0, \eta)$ and $a_i = a_{i0}$, where a_{i0} is given by the undisturbed ambient incident wave. On the longitudinal boundaries, $\eta = \pm\eta_0$, we assume the conditions $a_r = 0$, $\partial a_s / \partial \eta = \partial a_{s0} / \partial \eta$, and $\partial a_i / \partial \eta = 0$. Since $|a|$ is related to the wave amplitude $|A|$ by $|A| = (k/2\omega)^{1/2}|a|$, for clarity we present our results in terms of $|A|$.

As a numerical illustration, we consider a case with an ambient wave of $k_i \equiv |\mathbf{k}_i| = 3.48k_0$ and $\theta_i = 120^\circ$. From the resonance condition (2.5), we obtain that the third-order quartet resonance (with $\mathbf{k}_r = 2\mathbf{k}_i - \mathbf{k}_s$) occurs on the ray $\alpha = 7.5^\circ$. The resonance-generated wave has $k_r \equiv |\mathbf{k}_r| = 7.4k_0$ and $\theta_r = 127^\circ$ (cf. figure 2).

Figures 4(a) and 4(c) show the amplitude of the resonance-generated wave, $|A_r|$, for this case in the neighbourhood of the resonance ray $\alpha = 7.5^\circ$, viewed from centreline and far field, respectively. In the calculation, we use ambient wave steepness $\epsilon = 0.10$, and $k_{s0}A_0 = 0.18$. The numerical parameters used are $k_0\eta_0 = 400$, $k_0\xi_0 = 5$, and $k_0\Delta\xi = k_0\Delta\eta = 0.1$, where $\Delta\xi$ and $\Delta\eta$ are the discretization sizes in ξ and η , respectively. From figures 4(a) and 4(c), it is seen that $|A_r|$ grows monotonically with ξ in the very initial stage of the resonance (for $k_0(\xi - \xi_0)/2\pi = (\xi - \xi_0)/\lambda < \sim 25$), and then grows slowly in an oscillatory manner with a characteristic wavelength of $\sim 60\lambda$.

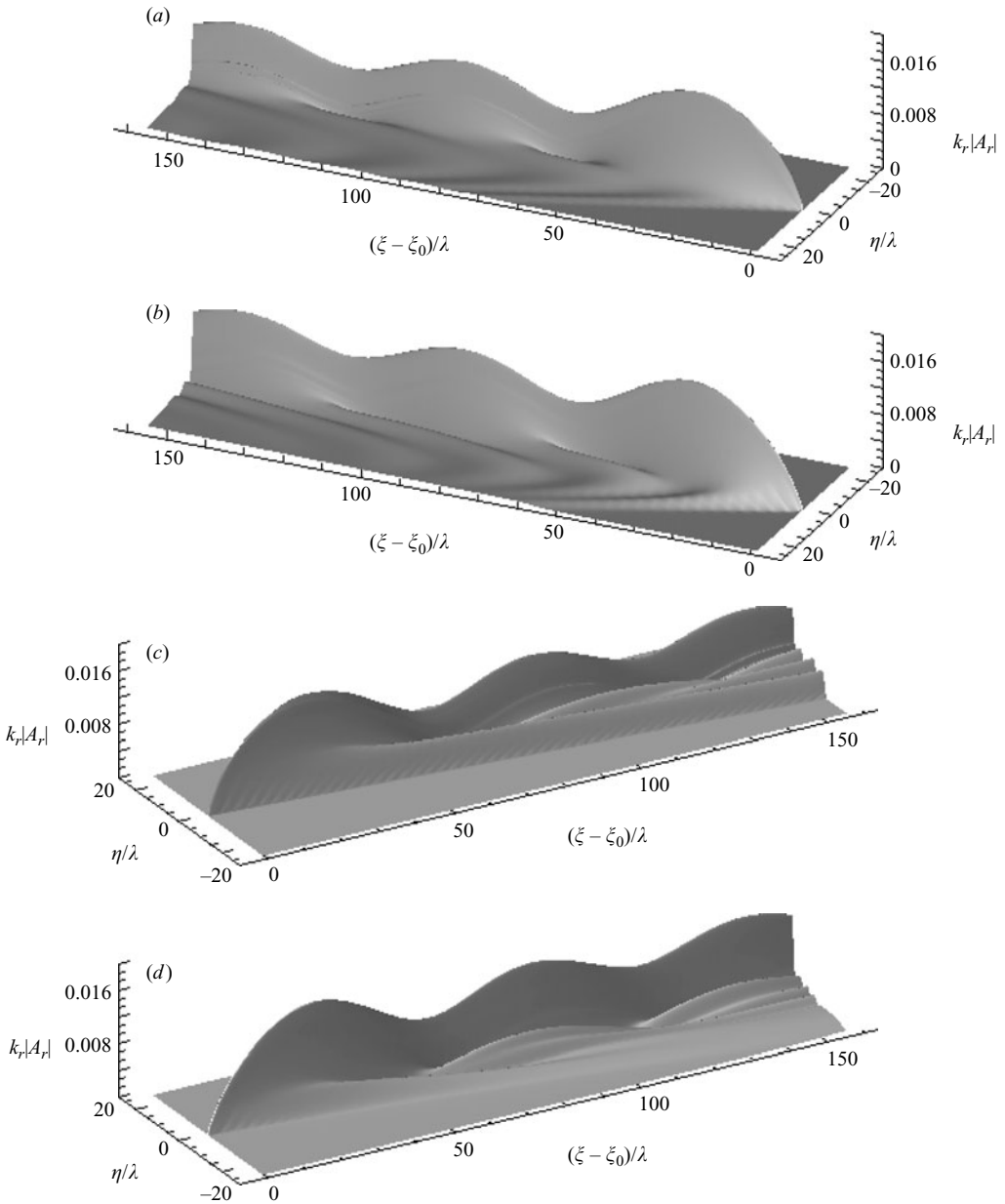


FIGURE 4. Amplitude envelope of the resonance-generated wave ($k_r = 7.4k_0$ and $\theta_r = 127^\circ$) in the neighbourhood of the resonance ray ($\alpha = 7.5^\circ$) in the Kelvin wake of a ship advancing in a plane ambient wave ($\epsilon = 0.10$, $k_i = 3.48k_0$, $\theta_i = 120^\circ$). The transverse ship wave steepness is $k_{s0}A_0 = 0.18$. The plots are made viewing from the centreline (*a*, *b*) and far field (*c*, *d*). The results were obtained using (*a*, *c*) the Zakharov equation model; and (*b*, *d*) the nonlinear Schrödinger equation.

In both near and far fields, $|A_r|$ decreases rapidly in the transverse direction as the distance from the resonance ray increases. For comparison, we also plot in figures 4(*b*) and 4(*d*) the corresponding result obtained using the NLS model (3.12). Comparing the two, it is seen that the two solutions agree relatively well on the resonance ray

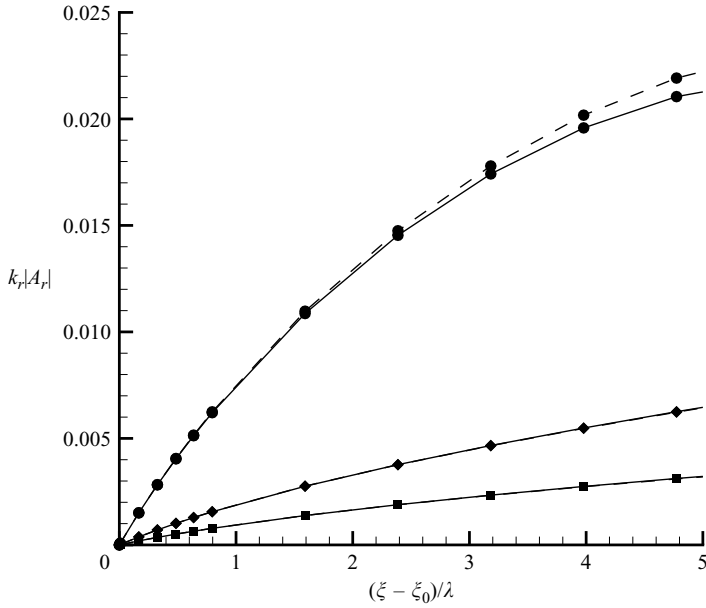


FIGURE 5. The initial growth of the resonance-generated wave along the resonance ray ($\eta = 0$) using the Zakharov equation model with $(k_{s0}A_0, \epsilon)$ begin given by $(0.09, 0.1)$, \blacksquare —; $(0.18, 0.1)$, \blacklozenge —; and $(0.18, 0.2)$, \bullet — . Also plotted are the results obtained by applying the nonlinear Schrödinger equation, with $(k_{s0}A_0, \epsilon)$ given by $(0.09, 0.1)$, $-\blacksquare-$; $(0.18, 0.1)$, $-\blacklozenge-$; and $(0.18, 0.2)$, $-\bullet-$. ($k_i = 3.48k_0$, $\theta_i = 120^\circ$, and $\alpha = 7.5^\circ$.)

$\eta = 0$, but deviate qualitatively as $|\eta|$ increases. This feature of the comparison is as expected since the NLS model does not include the detuning effect.

From the evolution equation (3.29), it is clear that at the initial stage of resonance where $|a_r|/|a_s| \ll 1$ and $|a_r|/|a_i| \ll 1$, the growth of $|a_r|$ is determined primarily by the cubic interaction term $T_{rsii}a_s^*a_i^2$. At this stage, it is reasonable to assume that $a_i \sim a_{i0}$ and $a_s \sim a_{s0}$ along the resonance ray ($\eta = 0$). Thus, we obtain from (3.29) that $|a_r| \sim \xi^{1/2}a_0a_{i0}^2$ at the initial stage of the resonance. This is confirmed in figure 5, where the initial growth of $|A_r|$ along the resonant ray is plotted for different ship and ambient wave steepnesses. Also plotted for comparison in the figure are the initial evolutions obtained from NLS. These results on the resonant ray are indistinguishable for the smaller steepness cases; and for the very large steepness case, the deviation is appreciable (only) with increasing resonance distance. The good performance of the NLS in this context can be expected, since for relatively small ambient and ship wave steepnesses and limited resonance growth (distance), the detuning along the resonance ray is small.

To illustrate the detuning effect further, we show in figure 6(a) a quantitative comparison of the two solutions for $|A_r|$ on the resonance ray ($\eta = 0$) over a long evolution distance for the same case shown in figure 4. Compared with the solution by the Zakharov equation model, the NLS solution overestimates $|A_r|$ in the far field (for $(\xi - \xi_0) > 15\lambda$), though the two solutions show a similar oscillatory feature. A more stringent comparison of the NLS, even for small evolution distance, is to compare the transverse variations of $|A_r|$ across the resonance ray. Figure 6(b) shows a typical result at distance $(\xi - \xi_0)/\lambda = 10$. The resonant wave amplitude is narrowly confined along the α_0 ($\eta = 0$) ray, decreasing to zero monotonically and rapidly

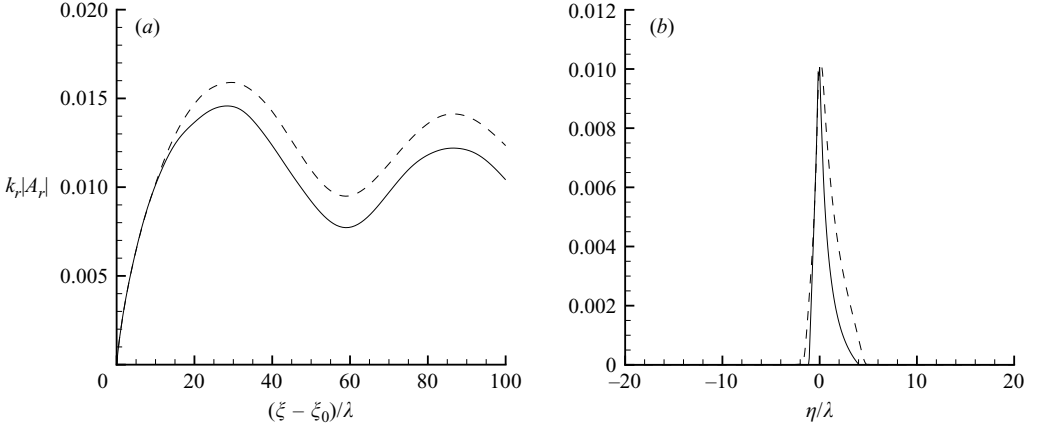


FIGURE 6. (a) Longitudinal variation of $|A_r|$ on the resonance ray ($\eta=0$), and (b) transverse variation of $|a_r|$ across the resonance ray at $(\xi - \xi_0)/\lambda=10$, obtained using the Zakharov equation model (—) and the nonlinear Schrödinger equation (- - -). ($k_i = 3.48k_0$, $\theta_i = 120^\circ$, $\alpha = 7.5^\circ$, $k_r = 7.4k_0$, $\theta_r = 127^\circ$, $\epsilon = 0.10$, and $k_{s0}A_0 = 0.18$.)

outboard ($\eta < 0$). On the inboard side (towards the ship's track, $\eta > 0$), the envelope is somewhat broader and the attenuation behaviour is more complex, displaying local minima/maxima (see also the comparison in figure 4). Compared with the NLS prediction, the maximum amplitude ($\eta \approx 0$) is well predicted (at this relatively small evolution distance), but the behaviours away from the resonance are not well captured, especially on the inboard side. These results indicate that the detuning effect is important and needs to be considered for accurately describing the features of the generated wave with long evolution distance and in the region away from the resonance ray.

Focusing on the results from the Zakharov evolution equations (3.29)–(3.31) from now on, we plot in figure 7 the longitudinal variation of $|A_r|$ along the resonance ray over a long evolution distance ξ for different ambient and ship wave steepnesses. The amplitude reaches an initial maximum over a distance that appears to depend primarily on ambient wave steepness, increasing approximately quadratically with decreasing ϵ . This feature of the solution is consistent with fact that the resonance in this case is dominated by the interaction term $T_{rsii}a_s^*a_i^2$. Beyond this maximum, $|A_r|$ oscillates and decreases slowly with increasing ξ . The wavelength of this oscillation increases with decreasing ϵ also almost quadratically, and appears to be insensitive to changing steepness of the transverse ship wave.

Across the resonance ray, $|A_r|$ displays a soliton-like variation (figure 6b). This behaviour is a result of the detuning effect. For the present resonance interaction problem, the detuning comes from two sources: one associated with imperfect satisfaction of the resonance condition away from the resonance ray, and the other with the amplitude modulation of the transverse ship wave across the resonance ray. To characterize the transverse extent or width in the η direction of the resonance-generated wave, we define the half-width of the envelope of $|A_r|$ as $W(\xi) = \eta_+ - \eta_-$, where η_{\pm} represent the positions where $\int_0^{\eta_+} |A_r|^2 d\eta = 0.5 \int_0^{\infty} |A_r|^2 d\eta$ and $\int_{\eta_-}^0 |A_r|^2 d\eta = 0.5 \int_{-\infty}^0 |A_r|^2 d\eta$. Clearly, W is the width within which half of the energy of the envelope is obtained. Figure 8 shows the result of $W(\xi)$ for different ambient and ship wave steepnesses. The results are consistent with those on the resonance ray $\eta=0$ in figure 7. W has a strong dependence on the ambient wave

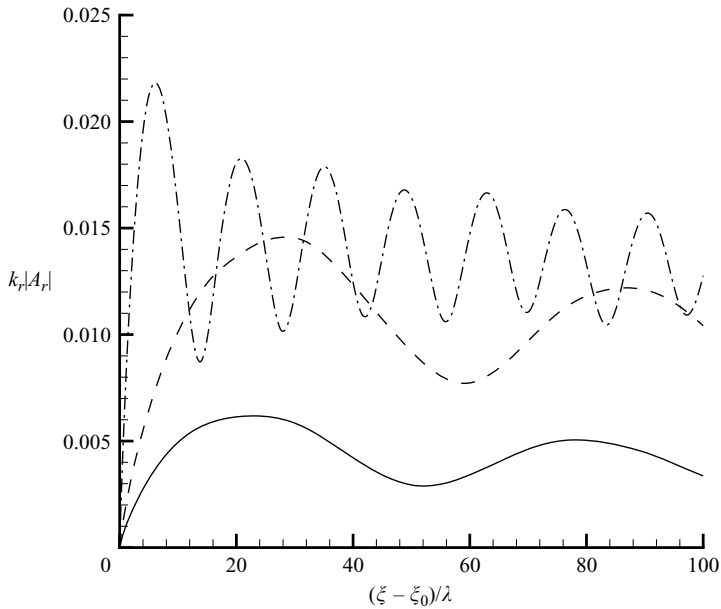


FIGURE 7. Longitudinal variation of the resonance-generated wave $|A_r|$ along the resonance ray with $(k_{s0}A_0, \epsilon)$ given by $(0.09, 0.1)$, —; $(0.18, 0.1)$, - - -; $(0.18, 0.2)$, — · —. ($k_i = 3.48k_0$, $\theta_i = 120^\circ$, and $\alpha = 7.5^\circ$.)

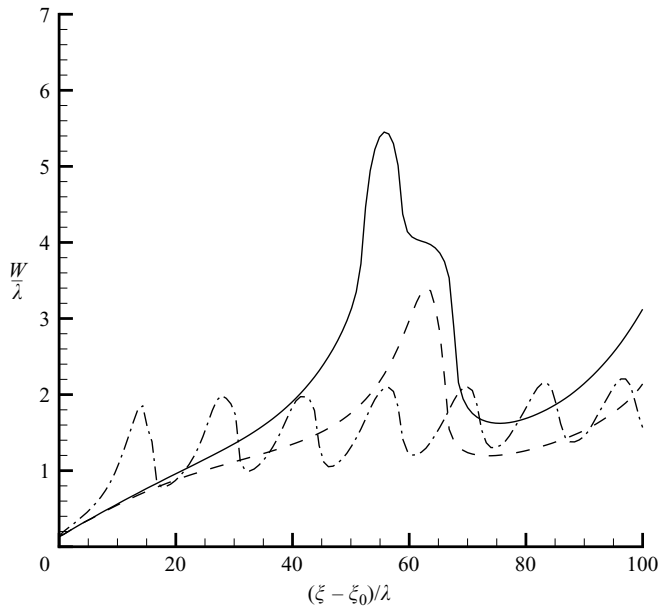


FIGURE 8. The half-width $W(\xi)$ of the envelope of the resonance-generated wave across the resonance ray with $(k_{s0}A_0, \epsilon)$ given by $(0.09, 0.1)$, —; $(0.18, 0.1)$, - - -; and $(0.18, 0.2)$, — · —. ($k_i = 3.48k_0$, $\theta_i = 120^\circ$, and $\alpha = 7.5^\circ$.)

steepness but is relatively insensitive to the ship wave steepness. Similarly, W also exhibits an oscillatory modulation in ξ with characteristic wavelength comparable to that for $|A_r|$ along the resonance ray (cf. figure 7).

4. Direct numerical simulations

We now turn to a direct numerical verification of our theoretical result. The nonlinear wave-wave interactions involving a full Kelvin wake and an ambient propagating wave is simulated using an efficient high-order spectral (HOS) method. The total wave field in the wake obtained from the direct nonlinear simulation contains different wave systems and components. These include the original (nonlinear) Kelvin ship and ambient waves, the locked waves due to nonlinear interactions of ship and ambient waves, and the resonance-generated wave with wave vector \mathbf{k}_r (in which we are primarily interested). Based on basic relations (in frequency and wave vector) of interacting wave components in the nonlinear wave system, the information of the resonance-generated wave is identified from the total wave field and is then compared with the theoretical prediction.

HOS is based on a Zakharov equation mode-coupling framework, but is generalized to include up to an arbitrary order M in wave steepness and a large number N of wave modes. The method obtains exponential convergence with N (and M) and computational effort only linearly proportional to N (e.g. Dommermuth & Yue 1987). Originally developed for nonlinear gravity wave interactions (Dommermuth & Yue 1987), HOS has since been extended to include the presence of moving atmospheric forcing (Dommermuth & Yue 1988), finite depth and depth variations (Liu & Yue 1998), and bodies (Liu, Dommermuth & Yue 1992; Zhu *et al.* 1999). The high efficiency and accuracy of HOS is well suited to the direct wave simulation of the present nonlinear resonant wave interaction problem.

For simplicity and without loss of generality, we consider the Kelvin waves generated by a moving dipole. A dipole of strength ϱ is located at a distance h below the mean free surface and moves forward in the $+X$ direction at speed U . For comparison to the theoretical result (in §3.4) in which only the transverse wave is involved, we consider the relatively deep submergence case ($k_0h \gg 1$) for which the transverse wave is dominant over the diverging wave (Newman 1987). For the ambient wave, we superimpose an exact (fully nonlinear) Stokes wave (Schwartz 1974) with wave vector satisfying the resonance conditions of §2. The (nonlinear) Kelvin waves as well as waves resulting from nonlinear interactions are allowed to develop in time via the HOS simulation.

In the numerical simulation, we choose a square (aligned with $X'-Y'$) computational domain with a side of length $L = 100/k_0$. The computational domain moves with the dipole at forward speed U such that the position of the dipole with respect to the computational domain is fixed. In the computations, we use $N = N_x \times N_y = 512 \times 512$ spectral wave modes and a time step $\Delta t = 0.05U/g$. To account for the third-order quartet resonant interactions among the waves, the HOS simulations are performed with order M up to 3. There are extensive validations of the HOS simulations. For brevity these are omitted here (for specific results of the present problem, see Dommermuth & Yue 1988; Zhu 2000).

We now show results for a specific resonant interaction case, for comparison with theory (in §3.4), with ambient wave $k_i = 3.48k_0$, $\theta_i = 120^\circ$ and steepness $\epsilon = 0.10$. For these values of k_i and θ_i , the theory predicts the generation of a resonant propagating wave with $k_r = 7.40k_0$ and $\theta_r = 127^\circ$ along the $\alpha = 7.5^\circ$ ray. For the moving dipole, we use a dipole strength $\varrho = 0.1U^7/g^3$ and submergence $k_0h = 7.0$. The simulation is terminated when the steady state or limit-cycle of the nonlinear wave field in the wake of the source is reached. From the nonlinear simulation, we examine the presence and characteristics of the resonance-generated wave in the wake. To obtain these from direct nonlinear simulations, we subtract the (nonlinear) steady Kelvin waves of the

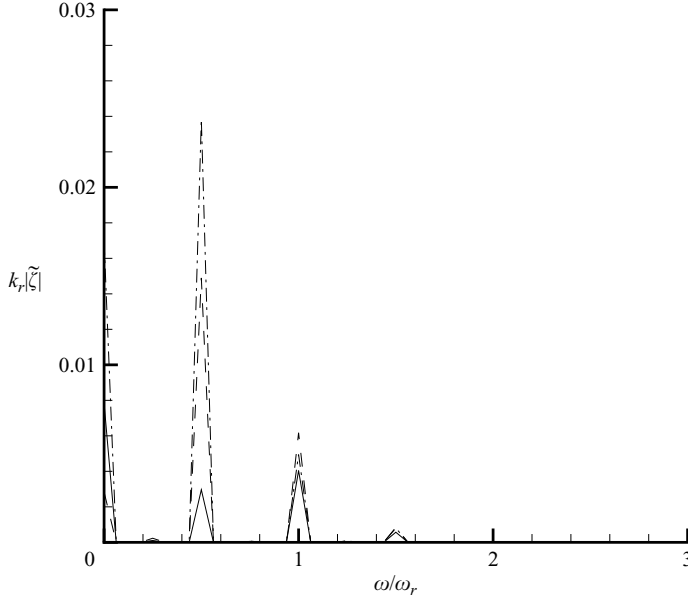


FIGURE 9. The frequency domain amplitude ($\tilde{\zeta}(\xi, 0, \omega)$) at three locations: $\xi = 2.3\lambda_0$ (—), $\xi = 4.6\lambda_0$ (- - -), and $\xi = 9.2\lambda_0$ (- · -). The dipole is located at $\xi = \eta = 0$ with a strength of $\varrho = 0.1U^7/g^3$ and a submergence of $k_0h = 7.0$.

dipole $\zeta_s(\xi, \eta)$ and the nonlinear ambient wave $\zeta_i(\xi, \eta, t)$ from the total nonlinear wave field $\zeta_{total}(\xi, \eta, t)$ to obtain

$$\zeta(\xi, \eta, t) = \zeta_{total}(\xi, \eta, t) - \zeta_s(\xi, \eta) - \zeta_i(\xi, \eta, t), \quad (4.1)$$

where ζ contains all the wave components associated with the nonlinear interactions between the Kelvin wave and the ambient wave. Up to third order, the wave vectors of these components are: $\mathbf{k}_i \pm \mathbf{k}_s$, $\mathbf{k}_i \pm \mathbf{k}_i \pm \mathbf{k}_s$ and $\mathbf{k}_i \pm \mathbf{k}_s \pm \mathbf{k}_s$.

On taking the Fourier transform of $\zeta(\xi, \eta, t)$ with respect to t , we obtain the amplitude of the interaction-generated waves in the frequency domain:

$$\tilde{\zeta}(\xi, \eta, \omega) = \frac{2}{nT_{re}} \int_{\tau_0}^{\tau_0 + nT_{re}} \zeta(X', Y', t) e^{i\omega_{re}t} dt, \quad (4.2)$$

where $T_{re} = 2\pi/\omega_{re} \equiv 2\pi/(\omega_r - \mathbf{U} \cdot \mathbf{k}_r)$ is the encounter period of the resonance-generated wave, n is an integer, and τ_0 a time interval selected so that limit-cycle values for (4.2) are obtained.

Figure 9 plots the spectrum of the interaction-generated waves $\tilde{\zeta}$ at three locations along the resonance ray. The peak at $\omega = 0$ corresponds to the third-order components $\mathbf{k}_i - \mathbf{k}_i \pm \mathbf{k}_s$ which have zero encounter frequency in the moving coordinate system. The second-order waves $\mathbf{k}_i \pm \mathbf{k}_s$, as well as the third-order components $\mathbf{k}_i \pm \mathbf{k}_s \pm \mathbf{k}_s$, have encounter frequency $\omega_{ie} \equiv \omega_i - \mathbf{U} \cdot \mathbf{k}_i$. The third-order waves $2\mathbf{k}_i \pm \mathbf{k}_s$ and the (small) fourth-order waves $2\mathbf{k}_i \pm 2\mathbf{k}_s$ share the frequency $2\omega_{ie}$. One notes that in HOS time-domain simulations with $M=3$, partial contributions to higher-order quantities can exist in the solution (see Liu, Dommermuth & Yue 1992 for detailed discussions).

To separate the resonance-generated wave $\mathbf{k}_r = 2\mathbf{k}_i - \mathbf{k}_s$ from the locked wave components with the same encountering frequency, we do a further Fourier transform of $\tilde{\zeta}(\xi, 0, \omega_{re})$ with respect to ξ . In spectral domain, $\tilde{\zeta}(\xi, 0, \omega_{re})$ becomes $\tilde{\zeta}(k, 0, \omega_{re})$,

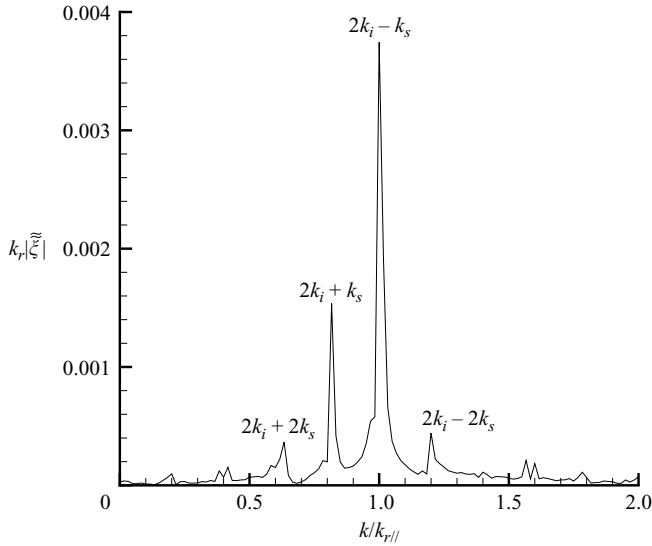


FIGURE 10. The Fourier transformation of the complex amplitude $\tilde{\zeta}(\xi, 0, \omega_{re})$ with respect to ξ , where $k_{r\parallel}$ is the component of \mathbf{k}_r parallel to the resonance ray. The dipole is located at $\xi = \eta = 0$ with a strength of $\varrho = 0.1U^7/g^3$ and a submergence of $k_0h = 7.0$.

which is plotted in figure 10. We see that it contains four main components which correspond to the resonance-generated wave $2\mathbf{k}_i - \mathbf{k}_s$, and the locked waves $2\mathbf{k}_i + \mathbf{k}_s$ and $2\mathbf{k}_i \pm 2\mathbf{k}_s$.

To extract the generated wave $\mathbf{k}_r = 2\mathbf{k}_i - \mathbf{k}_s$, we perform filtering in the spectral domain to eliminate the locked wave components to obtain $\tilde{\zeta}_r(k, 0, \omega_{re})$. This is the frequency-spectral domain representation of the generated wave \mathbf{k}_r along the resonance ray. An inverse Fourier transformation is finally performed to obtain the resonance-generated wave from the direct simulation, $\tilde{\zeta}_r(\xi, 0, \omega_{re})$, which has amplitude $|A_r| = |\tilde{\zeta}_r(\xi, 0, \omega_{re})|$. A similar procedure is applied to obtain $\tilde{\zeta}_r(\xi, \eta, \omega_{re})$ for values of $\eta \neq 0$.

Figure 11 plots the distribution of this amplitude $|A_r|$ in the wake. The existence of the resonance-generated wave along the predicted $\alpha = 7.5^\circ$ resonance ray is clearly seen. The amplitude as well as width of $|A_r|$ increase with downwave distance, in qualitative agreement with theory. Note that the filtering, first in frequency and then in the amplitude of the wave vector, applied to obtain figure 11, is designed specifically to extract $|A_r|$ along the resonance ray, so that information of $|A_r|$ in the figure away from the ray is not useful.

To make quantitative comparison with theory, we obtain the amplitude of the transverse wave at the starting point of the resonance by matching (3.34) to the simulated steady Kelvin wave elevation along the resonance ray. This is shown in figure 12, which shows a very good match with $k_{s0}A_0 = 0.067$ and $k_0\xi_0 = 5$. With this, we obtain finally quantitative comparison between theory and direct HOS simulation. Figure 13 shows this comparison for the initial growth of the resonant wave along the $\eta = 0$ ray. The comparison is quite satisfactory and offers a further independent validation of the theory (and the HOS simulation). We note here that the rapid oscillation in the direct simulation result is associated with the large $k_r \simeq 7.4k_0$, while the slower modulations are associated with the wave vectors of the

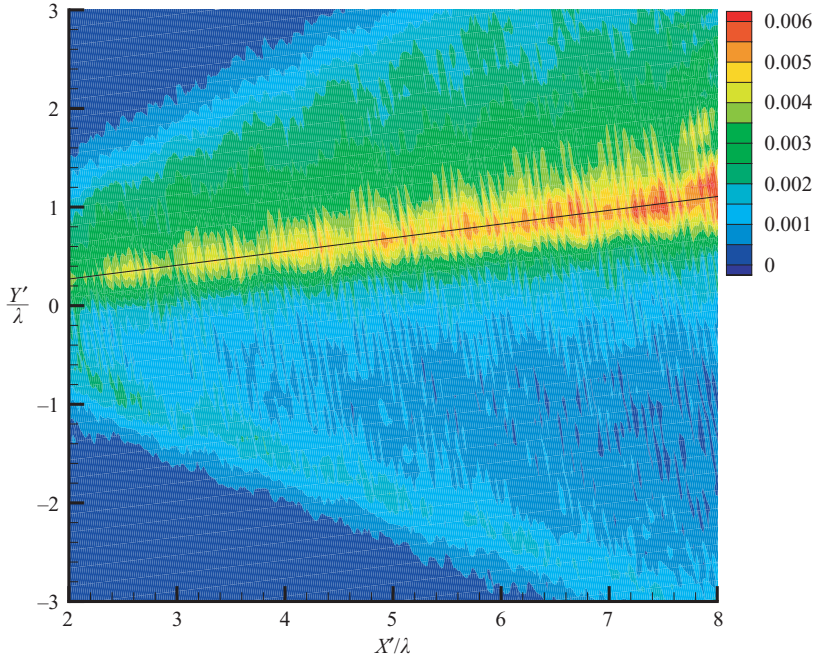


FIGURE 11. Amplitude of the generated progressive wave $k_r |A_r|$ in the wake of a submerged dipole (strength $\varrho = 0.1U^7/g^3$ and submergence $k_0 h = 7.0$). We plot the HOS simulation result with $\epsilon = 0.10$. The resonance ray ($\alpha = 7.5^\circ$) is shown with a solid line.

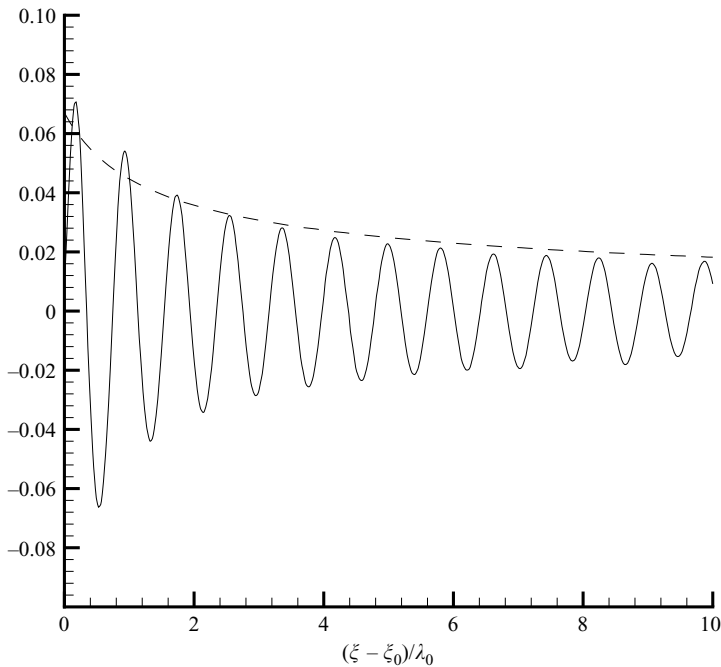


FIGURE 12. The HOS simulation result ($M = 3$) (—) of the Kelvin wave elevation $k_s \zeta$ of a moving point source along the resonant ray ($\alpha = 7.5^\circ$) and the matched envelope (- -) of the transverse wave based on equation (3.34) with $k_{s0} A_0 = 0.067$ and $k_0 \xi_0 = 5$. The dipole strength $\varrho = 0.1U^7/g^3$ and submergence $k_0 h = 7.0$.

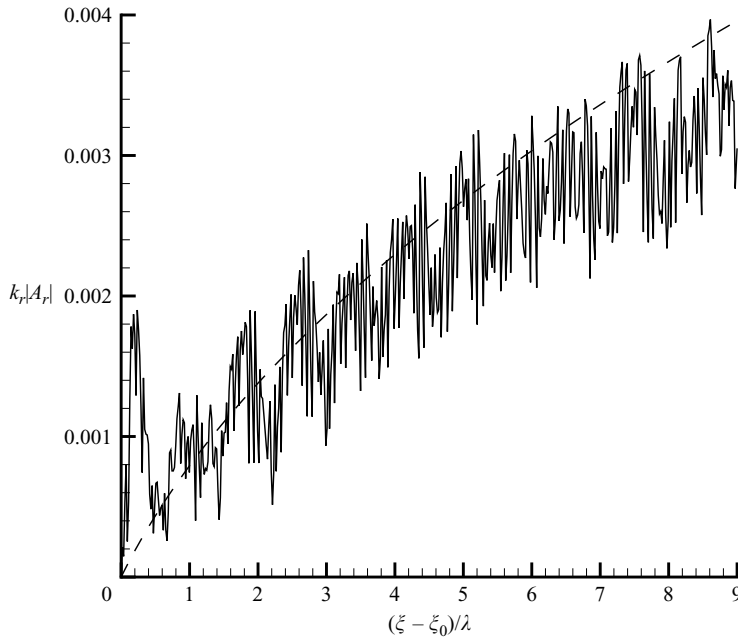


FIGURE 13. Comparison of the amplitude of the generated progressive wave on the resonance ray ($\alpha = 7.5^\circ$) in the wake of a submerged point dipole between the direct HOS simulation ($M = 3$) and the theoretical analysis. We plot the HOS simulation result with $\epsilon = 0.10$ and $k_{s0}A_0 = 0.067$ (—) and the theoretical prediction (---).

interacting components. The amplitude of the generated wave increases with the interaction distance ξ , while that of the ship wave decreases with ξ like $\xi^{-1/2}$ (cf. 3.34). As a result, their ratio $|A_r|/|A_s|$ increases (from zero) to 0.03 (with the ratio of the steepness $k_r|A_r|/k_s|A_s| = 0.2$) at $(\xi - \xi_0)/\lambda_0 = 8$. Direct comparison results have also been obtained for additional resonance cases involving different ambient wave parameters (see Zhu 2000). The results are similar to figure 13 and are not presented. In particular, the direct simulation numerical results obtain the behaviour that the growth rate increases quadratically with the ambient wave steepness, as predicted by theory.

In the above analysis and computations, the narrow-banded spread of the incident wave itself is not explicitly considered. The treatment under the Zakharov approach in the case of a narrow-banded incident wave (around k_i) is very similar. The final effect on the resonant wave is also similar to that due to the detuning of k_s (cf. figures 4, 6*b*, 11): a narrow spread of the resonant wave around k_r with comparable total energy.

5. Conclusions

We investigate nonlinear resonant interactions among the steady waves in the Kelvin wake of a ship with constant forward speed and an (unsteady) plane ambient wave. We identify the conditions under which third-order quartet interactions among the ship and ambient waves become resonant along specific rays in the ship wake specified by the wave vector of the incident wave (relative to the ship velocity). This resonance generates a new propagating wave which grows and develops along the resonance ray. The position of the resonance and the basic characteristics of the generated waves are completely determined by the ship speed and the wave vector of ambient waves.

We obtain the mechanism and evolution of this resonance analytically using the cubic Schrödinger equation and the Zakharov equation. The former is derived by a multiple-scale approach with the assumption of constant wave vectors with amplitude modulations across a resonance ray. The latter is obtained using a narrow-band asymptotic analysis based on the third-order Zakharov differential–integral equation including the detuning effect associated with the variation of the wave vector of ship waves. The two solutions compare reasonably well along the resonance ray as well as in the nearfield of the resonance where the detuning is negligible, but deviate qualitatively with increasing distance from the ray. Solutions of the evolution equations elucidate the characteristics of the resonance-generated waves, which manifest as persistent soliton-like envelopes across the resonance ray.

As a further verification of the theoretical results, we perform direct nonlinear simulations of this problem using an efficient high-order spectral method. The resonance-generated wave is obtained in the simulations with the basic characteristics and the (initial) growth of its amplitude comparing well with the predictions of the theory.

The question remains open as to whether the resonance phenomenon we show can be readily observed in a complex open ocean environment. The quartet resonance-generated wave, initially of higher order (third order), grows with distance and could in theory become comparable to other wave components in the ship wake. Significantly, this wave is characterized by a specific wave vector, ray angle, and amplitude variation with distance, all distinct from other wave components in the system. These salient features facilitate the identification/detection of this wave component from the complicated total wavefield. Our direct numerical simulation confirms that this is indeed the case for a problem involving a single ambient wave. The practical detection of such waves in a complex environment is not a main focus of this paper, but we believe that the elucidation of the features and characteristic of this resonance provides a basis for such detection.

We would like to acknowledge the comments and suggestions of Professor Chiang C. Mei on an early presentation of this work. This research is supported financially by grants from the Office of Naval Research.

Appendix. Derivation of the cubic nonlinear Schrödinger (NLS) equation

For $n \leq 3$, $F^{(n)}$, $G^{(n)}$ and $H^{(n)}$ in (3.6), (3.7) and (3.8) are given by

$$F^{(1)} = 0, \quad G^{(1)} = 0, \quad H^{(1)} = \phi_t^{(1)}, \quad (\text{A } 1)$$

$$\left. \begin{aligned} F^{(2)} &= -2(\phi_{xx_1}^{(1)} + \phi_{yy_1}^{(1)}), \\ G^{(2)} &= -[\zeta^{(1)}\Gamma_z\phi^{(1)} + (\phi_x^{(1)2} + \phi_y^{(1)2} + \phi_z^{(1)2})_t + 2\phi_{tt_1}^{(1)}], \\ H^{(2)} &= \phi_{t_1}^{(1)} + \phi_t^{(2)} + \zeta^{(1)}\phi_{zt}^{(1)} + \frac{1}{2}(\phi_x^{(1)2} + \phi_y^{(1)2} + \phi_z^{(1)2}), \end{aligned} \right\} \quad (\text{A } 2)$$

$$F^{(3)} = -\left[\left(\frac{\partial^2}{\partial x_1^2} + \frac{\partial^2}{\partial y_1^2} \right) \phi^{(1)} + 2(\phi_{xx_2}^{(1)} + \phi_{yy_2}^{(1)}) + 2(\phi_{xx_1}^{(2)} + \phi_{yy_1}^{(2)}) \right], \quad (\text{A } 3a)$$

$$\begin{aligned} G^{(3)} &= -\left[2\phi_{tt_2}^{(1)} + \phi_{tt_1}^{(1)} + 2\phi_{tt_1}^{(2)} + \zeta^{(1)}(\Gamma_z\phi^{(2)} + 2\phi_{zt_1}^{(1)}) + \zeta^{(2)}\Gamma_z\phi^{(1)} \right. \\ &\quad \left. + 2(\phi_x^{(1)}\phi_x^{(2)} + \phi_y^{(1)}\phi_y^{(2)} + \phi_z^{(1)}\phi_z^{(2)})_t + 2(\phi_x^{(1)}\phi_{x_1}^{(1)} + \phi_y^{(1)}\phi_{y_1}^{(1)})_t \right] \end{aligned}$$

$$\begin{aligned}
& + (\phi_x^{(1)2} + \phi_y^{(1)2} + \phi_z^{(1)2})_{t_1} + \frac{\zeta^{(1)2}}{2} \Gamma_{zz} \phi^{(1)} + \zeta^{(1)} (\phi_x^{(1)2} + \phi_y^{(1)2} + \phi_z^{(1)2})_{tz} \\
& + \frac{1}{2} \left(\phi_x^{(1)} \frac{\partial}{\partial x} + \phi_y^{(1)} \frac{\partial}{\partial y} + \phi_z^{(1)} \frac{\partial}{\partial z} \right) (\phi_x^{(1)2} + \phi_y^{(1)2} + \phi_z^{(1)2}) \Big], \quad (\text{A } 3b)
\end{aligned}$$

$$\begin{aligned}
H^{(3)} & = \phi_{t_2}^{(1)} + \phi_{t_1}^{(2)} + \phi_t^{(3)} + \zeta^{(1)} (\phi_{zt}^{(2)} + \phi_{zt_1}^{(1)}) + \zeta^{(2)} \phi_{zt}^{(1)} \\
& + \phi_x^{(1)} \phi_x^{(2)} + \phi_y^{(1)} \phi_y^{(2)} + \phi_z^{(1)} \phi_z^{(2)} + \phi_x^{(1)} \phi_{x_1}^{(1)} + \phi_y^{(1)} \phi_{y_1}^{(1)} \\
& + \frac{1}{2} \zeta^{(1)2} \phi_{zzt}^{(1)} + \frac{1}{2} \zeta^{(1)} (\phi_x^{(1)2} + \phi_y^{(1)2} + \phi_z^{(1)2})_z, \quad (\text{A } 3c)
\end{aligned}$$

where $\Gamma \equiv g\partial/\partial z + \partial^2/\partial t^2$. Without loss of generality, we rewrite the condition (2.3) in the form

$$\mathbf{k}_1 = s_2 \mathbf{k}_2 + s_3 \mathbf{k}_3 + s_4 \mathbf{k}_4, \quad \omega_1 = s_2 \omega_2 + s_3 \omega_3 + s_4 \omega_4, \quad (\text{A } 4)$$

where $s_2, s_3, s_4 = \pm 1$ depending on the sign combination in (2.3). We define, for convenience, a space-fixed Cartesian coordinate system ($o - xyz$) with the x -axis pointing in the direction of \mathbf{k}_1 and the z -axis upwards.

The first-order solution is the superposition of propagating waves which form a resonant quartet:

$$\phi^{(1)} = \sum_j^J -\frac{g}{2\omega_j} e^{k_j z} [iA_j e^{i\psi_j} + \text{c.c.}], \quad \zeta^{(1)} = \sum_j^J \frac{1}{2} [A_j e^{i\psi_j} + \text{c.c.}], \quad (\text{A } 5)$$

where $\psi_j \equiv \mathbf{k}_j \cdot \mathbf{x} - \omega_j t$, $j = 1, 2, 3, 4$, and the integer J denotes the number of distinctive wave components in the quartet. For example, $J = 4$ if all four waves in the quartet are different, while $J = 3$ if any two of the four waves are identical.

Let $\phi_1^{(n)}$, $F_1^{(n)}$ and $G_1^{(n)}$ be the terms in $\phi^{(n)}$, $F^{(n)}$ and $G^{(n)}$ containing the factor $e^{i\psi_1}$. In order for $\phi_1^{(n)}$ to be non-trivial, the following solvability condition must be satisfied (for any n):

$$\int_{-\infty}^0 F_1^{(n)} e^{k_1 z} dz = G_1^{(n)} / g. \quad (\text{A } 6)$$

Applying the condition (A 6) for $n = 2$, the second-order evolution equation for A_1 is obtained:

$$\frac{\partial A_1}{\partial t_1} + C_{g_1} \frac{\partial A_1}{\partial x_1} = 0, \quad (\text{A } 7)$$

where $C_{g_1} = (1/2)\omega_1/k_1$ is the group velocity of the wave component \mathbf{k}_1 . No resonance occurs at the second order. The solutions of $\phi^{(2)}$ and $\zeta^{(2)}$ containing the factor $e^{i(s_j \psi_j + s_\ell \psi_\ell)}$ can be obtained:

$$\phi_{j,\ell}^{(2)} = T_{j,\ell} A_j^{\gamma_j} A_\ell^{\gamma_\ell} e^{k_{j,\ell} z} e^{i(s_j \psi_j + s_\ell \psi_\ell)}, \quad (\text{A } 8)$$

$$\zeta_{j,\ell}^{(2)} = \left[\frac{i}{g} (s_j \omega_j + s_\ell \omega_\ell) T_{j,\ell} + \frac{k_j + k_\ell}{4} + \frac{g(k_j k_\ell - s_j s_\ell \mathbf{k}_j \cdot \mathbf{k}_\ell)}{2s_j s_\ell \omega_j \omega_\ell} \right] A_j^{\gamma_j} A_\ell^{\gamma_\ell} e^{i(s_j \psi_j + s_\ell \psi_\ell)}, \quad (\text{A } 9)$$

where

$$\begin{aligned}
k_j & = |\mathbf{k}_j|, \quad k_{j,\ell} = |s_j \mathbf{k}_j + s_\ell \mathbf{k}_\ell|, \quad j, \ell = 2, 3, 4 \\
T_{j,\ell} & = -\frac{ig^2 (s_j / \omega_j + s_\ell / \omega_\ell) (k_j k_\ell - s_j s_\ell \mathbf{k}_j \cdot \mathbf{k}_\ell)}{2[gk_{j,\ell} - (s_j \omega_j + s_\ell \omega_\ell)]}, \quad j, \ell = 2, 3, 4.
\end{aligned}$$

When $s_j = 1$, $A_j^{\gamma_j} = A_j$ while $A_j^{\gamma_j} = A_j^*$ for $s_j = -1$.

The third-order evolution equation for A_1 is obtained by applying the condition (A 6) to $F_1^{(3)}$ and $G_1^{(3)}$. As expected, this evolution equation is identical to the two-dimensional cubic Schrödinger equation (see Mei *et al.* 2005) except for cubic terms representing the interactions with other waves in the quartet, which appear in $G_1^{(3)}$. In terms of ψ_j , these resonant cases are: $\psi_1 = \psi_1 + \psi_j - \psi_j$ and $\psi_1 = s_2\psi_2 + s_3\psi_3 + s_4\psi_4$. We have

$$G_1^{(3)} = ig \sum_j^J e^{i(\psi_1 + \psi_j - \psi_j)} C_{1,j,-j} |A_j|^2 A_1 + ig e^{i(s_2\psi_2 + s_3\psi_3 + s_4\psi_4)} C_{2,3,4} A_2^{\gamma_2} A_3^{\gamma_3} A_4^{\gamma_4} \quad (\text{A } 10)$$

where the coefficients $C_{2,3,4}$ and $C_{1,j,-j}$ are given by (A 13) below.

Applying the solvability condition (A 6) for $n = 3$, we obtain:

$$\left(\frac{\partial A_1}{\partial t_2} + C_{g_1} \frac{\partial A_1}{\partial x_2} \right) + i \left\{ \frac{\omega_1}{8k_1^2} \left(\frac{\partial^2 A_1}{\partial x_1^2} - 2 \frac{\partial^2 A_1}{\partial y_1^2} \right) + \sum_j^J C_{1,j,-j} |A_j|^2 A_1 + C_{2,3,4} A_2^{\gamma_2} A_3^{\gamma_3} A_4^{\gamma_4} \right\} = 0. \quad (\text{A } 11)$$

Combining (A 11) with (A 7), the evolution equation for A_1 is finally obtained:

$$\left(\frac{\partial A_1}{\partial t} + C_{g_1} \frac{\partial A_1}{\partial x} \right) + i \left\{ \frac{\omega_1}{8k_1^2} \left(\frac{\partial^2 A_1}{\partial x^2} - 2 \frac{\partial^2 A_1}{\partial y^2} \right) + \sum_j^J C_{1,j,-j} |A_j|^2 A_1 + C_{2,3,4} A_2^{\gamma_2} A_3^{\gamma_3} A_4^{\gamma_4} \right\} = 0, \quad (\text{A } 12)$$

where $A_j^{\gamma_j} = A_j$, $j=2,3,4$, for $s_j = 1$ and $A_j^{\gamma_j} = A_j^*$ for $s_j = -1$. The coefficient $C_{2,3,4}$ takes the form

$$\begin{aligned} C_{2,3,4} = & \left\{ -i(s_2\omega_2 + s_3\omega_3 + s_4\omega_4) \left[(k_2k_{3,4} - s_2\mathbf{k}_2 \cdot (s_3\mathbf{k}_3 + s_4\mathbf{k}_4)) \frac{T_{3,4}}{\omega_2} \right. \right. \\ & + (k_3k_{2,4} - s_3\mathbf{k}_3 \cdot (s_2\mathbf{k}_2 + s_4\mathbf{k}_4)) \frac{T_{2,4}}{s_3\omega_3} + (k_4k_{2,3} - s_4\mathbf{k}_4 \cdot (s_2\mathbf{k}_2 + s_3\mathbf{k}_3)) \frac{T_{2,3}}{s_4\omega_4} \left. \right] \\ & - \frac{g}{4} \left[(k_2 + k_3) \left(\frac{1}{s_2\omega_2} + \frac{1}{s_3\omega_3} \right) (k_2k_3 - s_2s_3\mathbf{k}_2 \cdot \mathbf{k}_3) \right. \\ & + (k_2 + k_4) \left(\frac{1}{s_2\omega_2} + \frac{1}{s_4\omega_4} \right) (k_2k_4 - s_2s_4\mathbf{k}_2 \cdot \mathbf{k}_4) \\ & \left. + (k_3 + k_4) \left(\frac{1}{s_3\omega_3} + \frac{1}{s_4\omega_4} \right) (k_3k_4 - s_3s_4\mathbf{k}_3 \cdot \mathbf{k}_4) \right] \\ & - \frac{g^2}{8s_2s_3s_4\omega_2\omega_3\omega_4} [((k_2 + k_3)k_4 - s_4(s_2\mathbf{k}_2 + s_3\mathbf{k}_3) \cdot \mathbf{k}_4)(k_2k_3 - s_2s_3\mathbf{k}_2 \cdot \mathbf{k}_3) \\ & + ((k_2 + k_4)k_3 - s_3(s_2\mathbf{k}_2 + s_4\mathbf{k}_4) \cdot \mathbf{k}_3)(k_2k_4 - s_2s_4\mathbf{k}_2 \cdot \mathbf{k}_4) \\ & + ((k_3 + k_4)k_2 - s_2(s_3\mathbf{k}_3 + s_4\mathbf{k}_4) \cdot \mathbf{k}_2)(k_3k_4 - s_3s_4\mathbf{k}_3 \cdot \mathbf{k}_4)] \\ & + \frac{i}{2g} [(gk_{2,3} - (s_2\omega_2 + s_3\omega_3)^2)k_{2,3}T_{2,3} + (gk_{2,4} - (s_2\omega_2 + s_4\omega_4)^2)k_{2,4}T_{2,4} \\ & \left. + (gk_{3,4} - (s_3\omega_3 + s_4\omega_4)^2)k_{3,4}T_{3,4}] \right\} \delta_{2,3,4}, \quad (\text{A } 13) \end{aligned}$$

where $\delta_{2,3,4} = 1/2$ if $s_2\mathbf{k}_2 \neq s_3\mathbf{k}_3 \neq s_4\mathbf{k}_4$, and otherwise, $\delta_{2,3,4} = 1$. In (A 12), the coefficients $C_{1,j,-j}$, $j = 1, 2, 3, 4$, can be determined from (A 13) by replacing $(s_2, s_3, s_4, \mathbf{k}_2, \mathbf{k}_3, \mathbf{k}_4, \omega_2, \omega_3, \omega_4)$ with $(1, 1, -1, \mathbf{k}_1, \mathbf{k}_j, \mathbf{k}_j, \omega_1, \omega_j, \omega_j)$, respectively.

The evolution equation for A_2 can be obtained from the above result by exchanging \mathbf{k}_1 and \mathbf{k}_2 and replacing s_2 by s_1 with the x -axis pointing in the direction of \mathbf{k}_2 . The solutions for A_3 and A_4 can also be obtained similarly.

REFERENCES

- AKYLAS, T. R. 1987 Unsteady and nonlinear effects near the cusp lines of the Kelvin ship-wave pattern. *J. Fluid Mech.* **175**, 333–342.
- BENNY, D. J. 1962 Nonlinear gravity wave interactions. *J. Fluid Mech.* **14**, 577–589.
- BENNY, D. J. & ROSKES, G. 1969 Wave instabilities. *Stud. Appl. Maths* **48**, 377–385.
- BOOIJ, N., RIS, R. C. & HOLTHUIJSEN, L. H. 1999 A third-generation wave model for coastal regions. Part 1. Model description and validation. *J. Geophys. Res.* **104**, 7649–7666.
- BROWN, E. D., BUCHSBAUM, S. B., HALL, R. E., PENHUM, J. P., SCHMITT, K. F., WATSON, K. M. & WYATT, D. C. 1989 Observations of nonlinear solitary wave packet in the Kelvin wake of a ship. *J. Fluid Mech.* **204**, 263–293.
- CAO, Y. 1991 Computation of nonlinear gravity waves by a desingularized boundary integral method. PhD thesis, University of Michigan.
- CRAWFORD, D. R., LAKE, B. M., SAFFMAN, P. G. & YUEN, H. C. 1981 Stability of weakly nonlinear deep-water waves in two and three dimensions. *J. Fluid Mech.* **105**, 177–191.
- DOMMERMUTH, D. G. & YUE, D. K. P. 1987 A high-order spectral method for the study of nonlinear gravity waves. *J. Fluid Mech.* **184**, 267–288.
- DOMMERMUTH, D. G. & YUE, D. K. P. 1988 The nonlinear three-dimensional waves generated by a moving surface disturbance. In *Proc. 17th Symp. on Naval Hydro., Hague, Netherlands*.
- EGGERS, K. & SCHULTZ, W. W. 1992 Investigation on time-harmonic disturbances for inner-Kelvin-angle wave packets. In *7th International Workshop on Water Waves and Floating Bodies*. Val de Reuil, France.
- FU, L. L. & HOLT, B. 1982 SESAT view of oceans and sea ice with synthetic aperture radar. *Jet Propulsion Lab. Publ.* 81–120.
- HALL, H. & BUCHSBAUM, S. 1990 A model for the generation and evolution of an inner-angle soliton in a Kelvin wake. In *Proc. 18th ONR Symp. Naval Hydrodynamics*, pp. 453–463.
- HASSELMANN, S., HASSELMANN, K., BAUER, E., JANSSEN, P. A. E. M., KOMEN, G. J., BERTOTTI, L., LIONELLO, P., GUILLAUME, A., CARDONE, V. C., GREENWOOD, J. A., REISTAD, M., ZAMBRESKY, L. & EWING, J. A. 1988 The WAM model: A third generation ocean wave prediction model. *J. Phys. Oceanogr.* **18**, 1775–1810.
- KRASITSKII, V. P. 1994 On reduced equation in the Hamiltonian theory of weakly nonlinear surface waves. *J. Fluid Mech.* **272**, 1–20.
- LI, J. J. & TULIN, M. P. 1999 On the stability and nonlinear dynamics of ocean-like wave systems with energy continuously distributed in direction. *J. Engng Maths* **35**, 59–70.
- LIU, Y., DOMMERMUTH, D. G. & YUE, D. K. P. 1992 A high-order spectral method for nonlinear wave-body interactions. *J. Fluid Mech.* **245**, 115–136.
- LIU, Y. & YUE, D.K.P. 1998 On generalized Bragg scattering of surface waves by bottom ripples. *J. Fluid Mech.* **356**, 297–356.
- MEI, C. C., STIASSNIE, M. & YUE, D. K. P. 2005 *Theory and Applications of Ocean Surface Waves*. World Scientific.
- MEI, C. C. & NACIRI, M. 1991 Note on ship oscillations and wake solitons. *Proc. R. Soc. Lond. A* **432**, 535–546.
- MUNK, W. H., SCULLY-POWER, P. & ZACHARIASEN, F. 1987 Ships from space. *Proc. R. Soc. Lond. A* **412**, 231–254.
- NEWMAN, J. N. 1971 Third order interactions in the Kelvin ship wave systems. *J. Ship Res.* **15**, 1–10.
- NEWMAN, J. N. 1977 *Marine Hydrodynamics*. The MIT Press.
- NEWMAN, J. N. 1987 Evaluation of the wave-resistance Green function. Part 1. The double integral. *J. Ship Res.* **31**, 79–90.

- NEWMAN, J. N. 1992 The Green function for potential flow in a rectangular channel. *J. Engng Math.* **26**, 51–59.
- PEREGRINE, D. H. 1971 A ship's waves and its wake. *J. Fluid Mech.* **49**, 353–360.
- PHILLIPS, O. M. 1960 Unsteady gravity waves of finite amplitude. Part 1. The elementary interactions. *J. Fluid Mech.* **9**, 193–217.
- REED, A. M. & MILGRAM, J. H. 2002 Ship wakes and their radar images. *Annu. Rev. Fluid Mech.* **34**, 469–502.
- SCHWARTZ, L. W. 1974 Computer extension and analytic continuation of Stokes' expansion for gravity waves. *J. Fluid Mech.* **62**, 553–578.
- SHEMDIN, O. 1987 SAR imaging of ship wakes in the gulf of Alaska. Report, Jet Propulsion Lab.
- TULIN, M. & MILOH, T. 1990 Ship internal waves in a shallow thermocline: the supersonic case. *Proc. 18th Symp. Naval Hydrodynamics*.
- YUE, D. K. P. & MEI, C. C. 1980 Forward diffraction of Stokes waves by a thin wedge. *J. Fluid Mech.* **99**, 33–52.
- ZAKHAROV, V. E. 1968 Stability of periodic waves of finite amplitude on the surface of a deep fluid. *J. Appl. Mech. Tech. Phys.* **9**, 190–194 (English translation.)
- ZHU, Q. 2000 Features of nonlinear wave-wave and wave-body interactions. PhD Thesis, Massachusetts Institute of Technology.
- ZHU, Q., LIU, Y., TJARAVAS, A. A., YUE, D. K. P. & TRIANTAFYLLOU, M. S. 1999 Mechanics of nonlinear short-wave generation by a moored near-surface buoy. *J. Fluid Mech.* **381**, 305–335.